Low temperature and timing properties of SIPMs

G.Collazuol
University of Padova and INFN

Overview
- Introduction
- Low T features, measurements, issues
- Timing features, measurements, issues
- Conclusions

Introduction: building block of a SiPM → GM-APD

Diode reverse-biased above $V_{breakdown}$

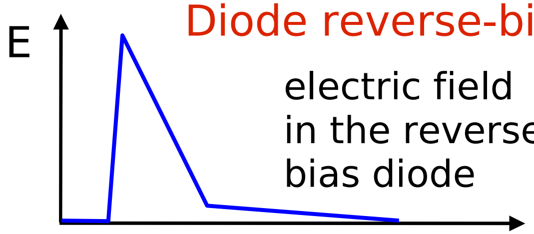

- t=0: carrier initiates the avalanche

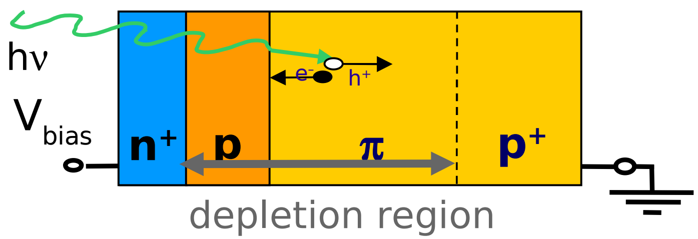

- $0<t<t_1$: avalanche spreading

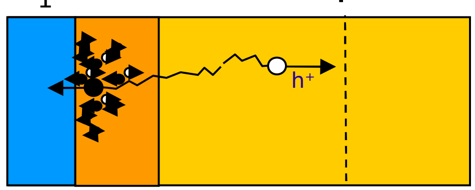

- $t_1<t$: self-sustaining current (limited by series R)

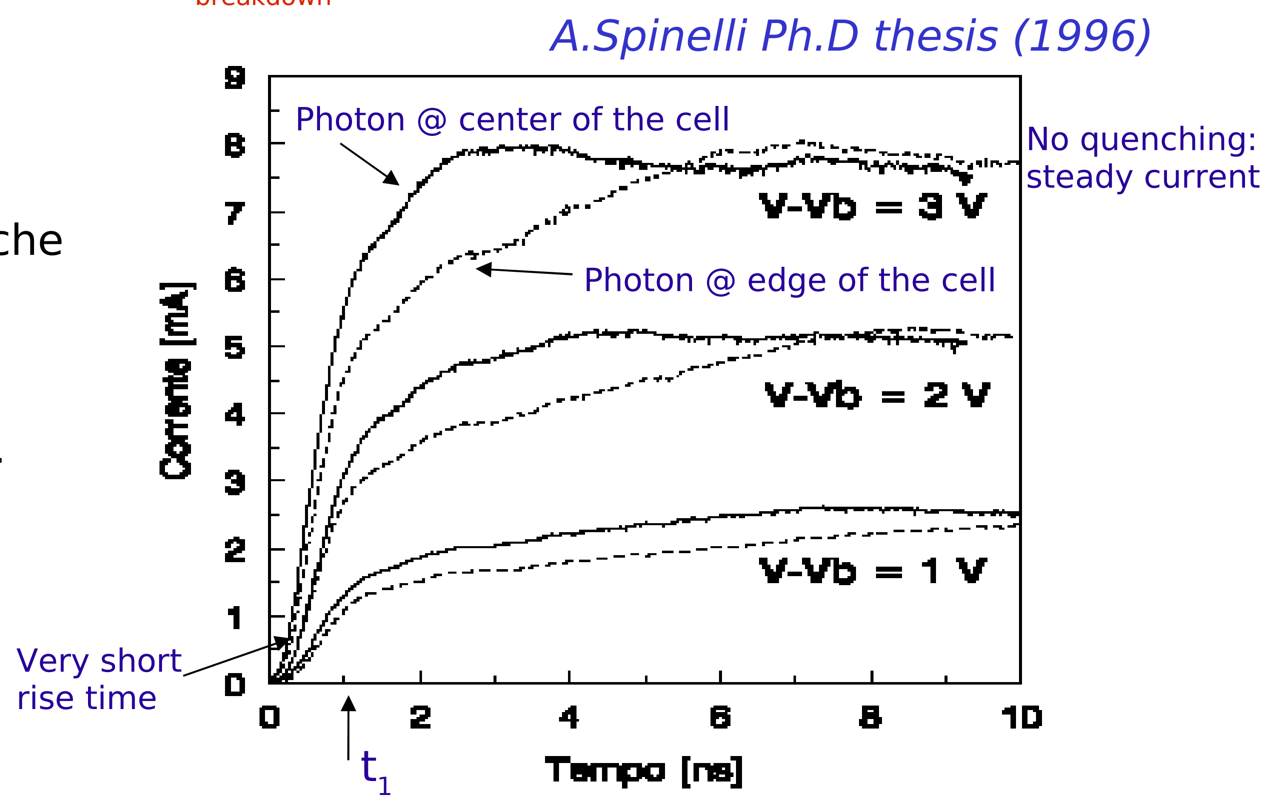

Avalanche processes in Si: studied since +50ys and widely exploited...
... not understood in the very detail

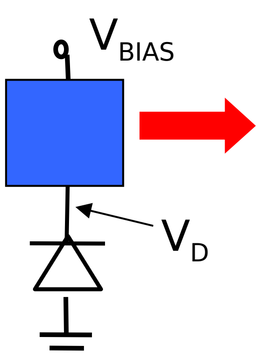

To detect another photon need a quenching mechanism. Two solutions:

- large resistance: passive quenching
- analog circuit: active quenching

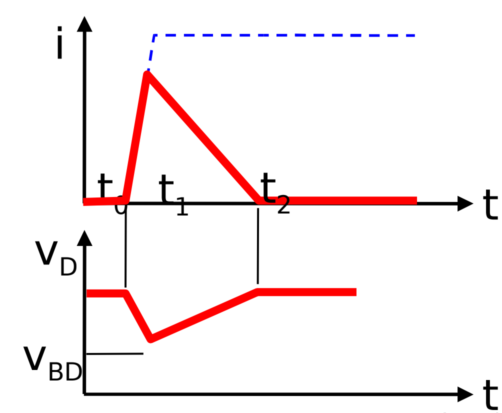

Reference - SiPM diode FBK

Shallow-Junction

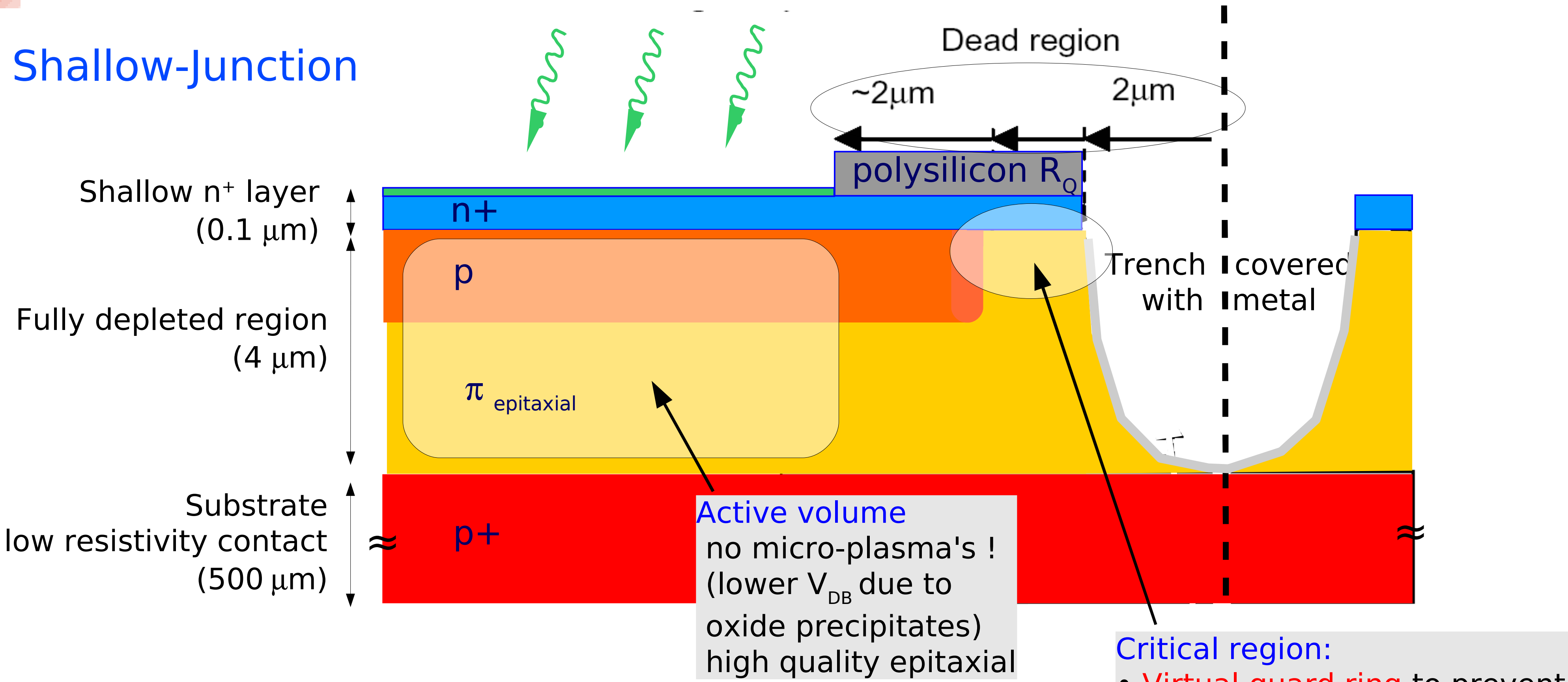

Optimization for the blue light (420nm)

- n^+ on p abrupt junction structure
- Anti-reflective coating (ARC) optimized for λ~420nm
- Very thin (100nm) n^+ layer: "low" doping n^+ layer
  → minimize Auger and SHR recombination
- Thin high-field region: "high" doping p layer (limited by tunneling breakdown)
  → fixes V_{BD} junction well below V_{BD} at edge
- R_Q by doped polysilicon
- Trenches for optical insulation (low cross-talk)
- Fill factor: 20% - 80%

C.Piemonte NIM A 568 (2006) 224

Operation principle of a GM-APD

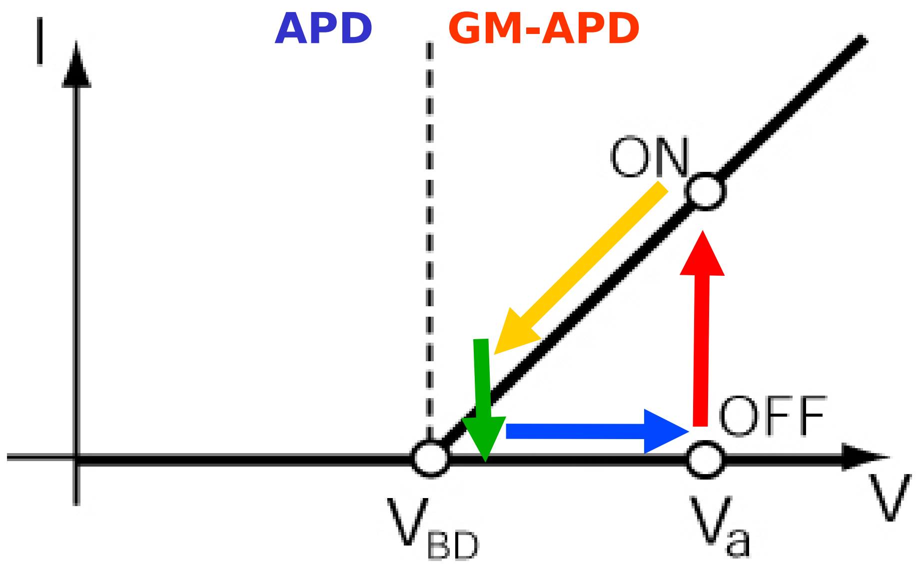

Haitz JAP 35 (1964)

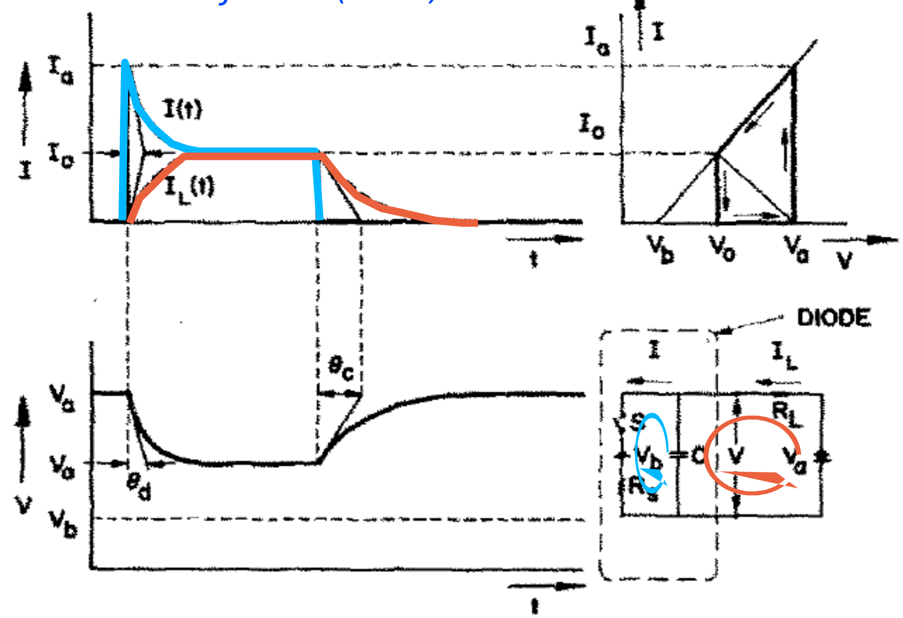

FIG. 3. Shape of current pulse for $\theta_d \ll \tau_1(I_0)$.

OFF condition: avalanche quenched, switch open, capacitance charged until no current flowing from V_{BD} to V_{BIAS} with time constant $R_q x C_d = \tau_{Quenching}$ (→ recovery time)

P_{01} = turn-on probability
probability that a carrier traversing the high-field region triggers the avalanche

P_{10} = turn-off probability
probability that the number of carriers traversing the high-field region fluctuates to 0

ON condition: avalanche triggered, switch closed
C_d discharges to V_{BD} with a time constant $R_d x C_d = \tau_{discharge}$,
at the same time the external current asymptotic grows to $(V_{bias}-V_{bd})/(R_q+R_d)$

Signal shape, Gain and Recovery time

Fast Capacitor (cell) discharge and slow recharge (roughly speaking)

If R_q is high enough the internal current decreases at a level such that statistical fluctuations quench the avalanche: need $i_{latch} \sim \Delta V/(R_q+R_d) \sim 10\mu A$

"Overvoltage"
$\Delta V \equiv (V_{bias}-V_{Breakdown})$

With usual R_q values turn-off time is very short O(1ns)

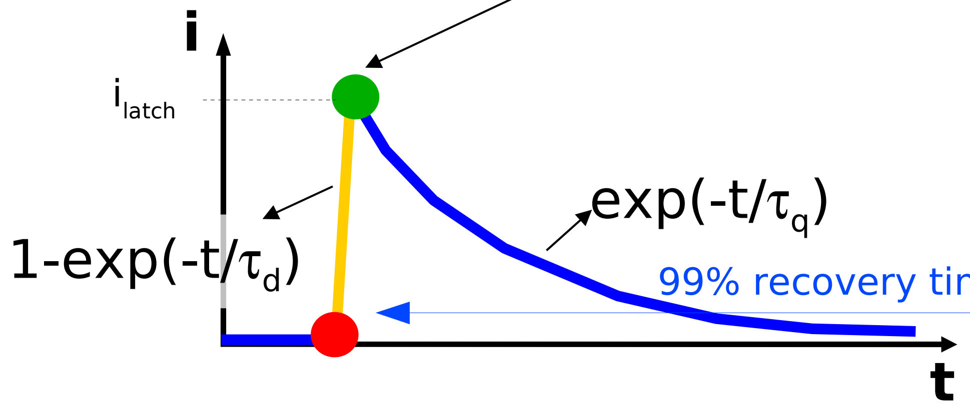

Rise time: $\tau_d = R_d C_d$ $\ll$ Falling time (recovery): $\tau_q = R_q C_d$

Recovery time: increases at low T due to polysilicon R_q while C_d is independent of T

also rise time expected to be T dependent (silicon R_d vs T)

Gain~C_d ΔV → independent of T

at fixed Over-Voltage (ΔV)

SiPM equivalent circuit (detailed model)

Single cell model → $(R_d||C_d)+(R_q||C_q)$

SiPM + load → $(||Z_{cell})||C_{grid} + Z_{load}$

Signal = slow pulse ($\tau_{d\ (rise)}, \tau_{q\text{-}slow\ (fall)}$) +
+ fast pulse ($\tau_{d\ (rise)}, \tau_{q\text{-}fast\ (fall)}$)

- $\tau_{d\ (rise)} \sim R_d(C_q+C_d)$
- $\tau_{q\text{-}fast\ (fall)} = R_{load}\ C_{tot}$ (fast; parasitic spike)
- $\tau_{q\text{-}slow\ (fall)} = R_q\ (C_q+C_d)$ (slow; cell recovery)

F.Corsi, et al. NIM A572 (2007)

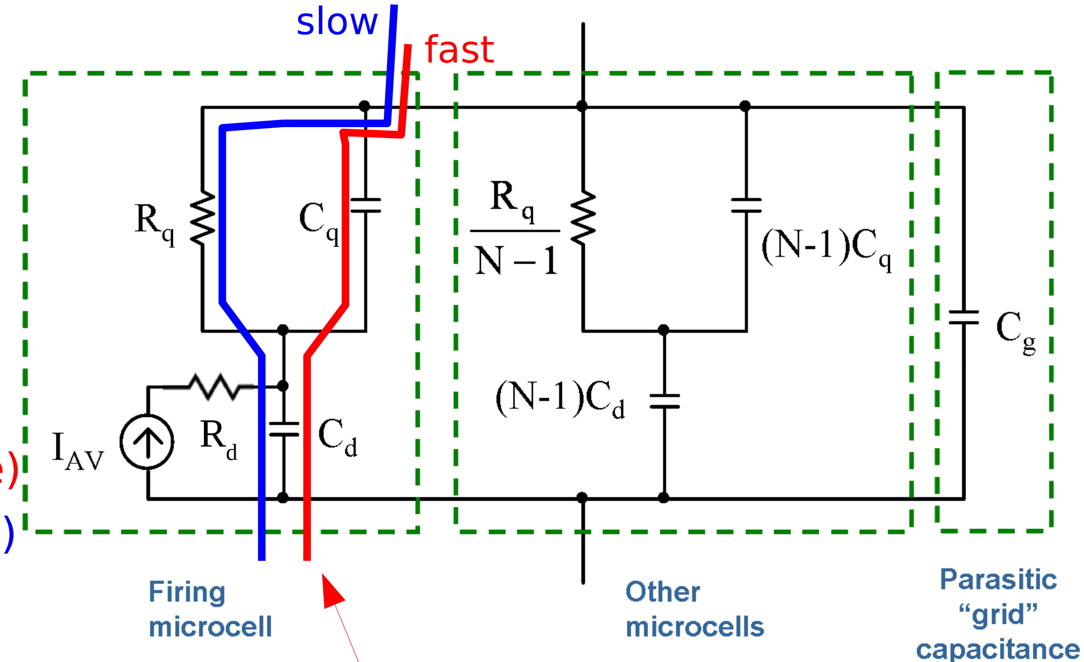

Cq → fast current supply path in the beginning of avalanche

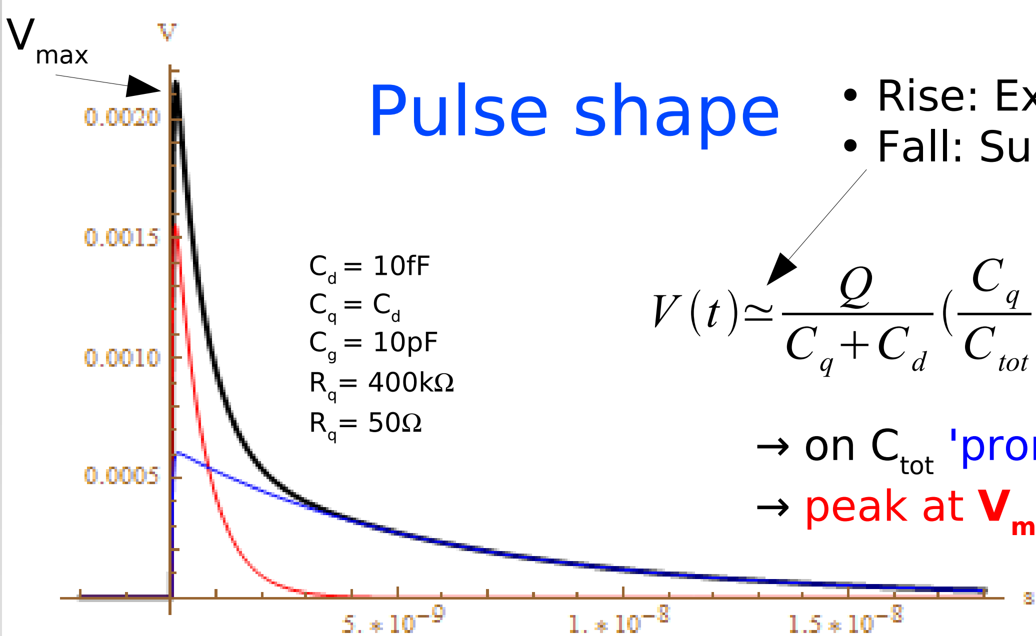

Pulse shape

- Rise: Exponential → Sp.Charge R x Cd,q; further filtered by parasitic inductance, stray C, ... (Low Pass)
- Fall: Sum of 2 exponentials

$$V(t) \simeq \frac{Q}{C_q+C_d}\left(\frac{C_q}{C_{tot}} e^{\frac{-t}{\tau_{FAST}}} + \frac{R_{load}}{R_q}\frac{C_d}{C_q+C_d} e^{\frac{-t}{\tau_{SLOW}}}\right)$$

→ on C_{tot} 'prompt' charge $\mathbf{Q_{fast} = Q\ C_q/(C_q+C_d)}$

→ peak at $\mathbf{V_{max} \sim Q_{fast}/C_{tot}}$ **is independent of $\mathbf{R_{load}}$**

Pulse shape: dependence on Temperature

Single cell model → $(R_d||C_d)+(R_q||C_q)$
SiPM + load → $(||Z_{cell})||C_{grid} + Z_{load}$

Signal = slow pulse ($\tau_{d\,(rise)}, \tau_{q\text{-}slow\,(fall)}$) +
+ fast pulse ($\tau_{d\,(rise)}, \tau_{q\text{-}fast\,(fall)}$)

- $\tau_{d\,(rise)} \sim R_d(C_q+C_d)$
- $\tau_{q\text{-}fast\,(fall)} = R_{load}\ C_{tot}$ (fast; parasitic spike)
- $\tau_{q\text{-}slow\,(fall)} = R_q\,(C_q+C_d)$ (slow; cell recovery)

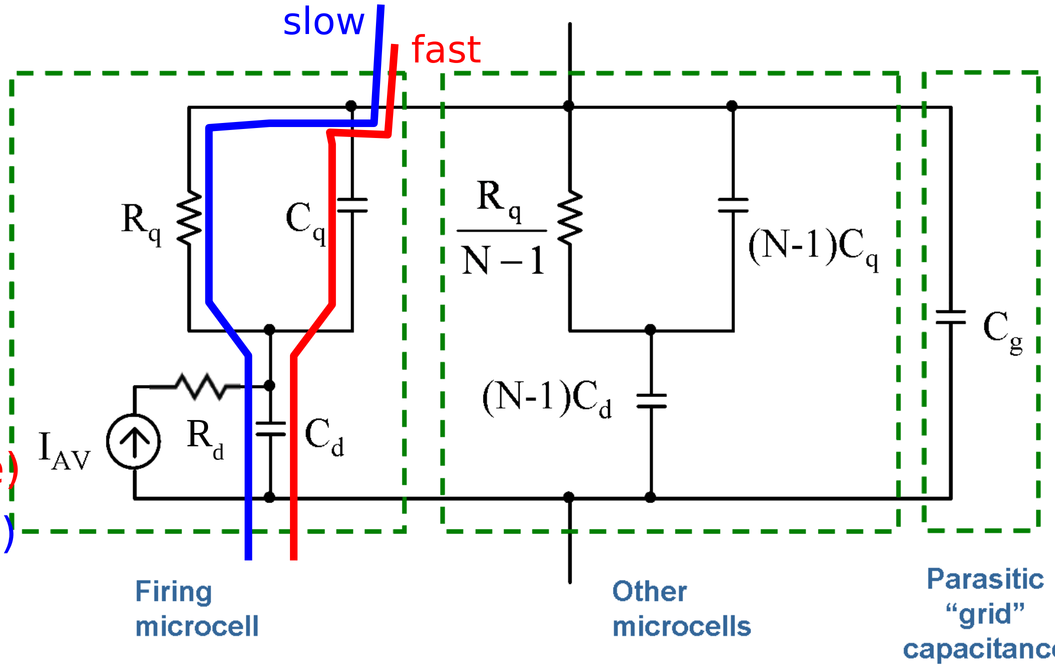

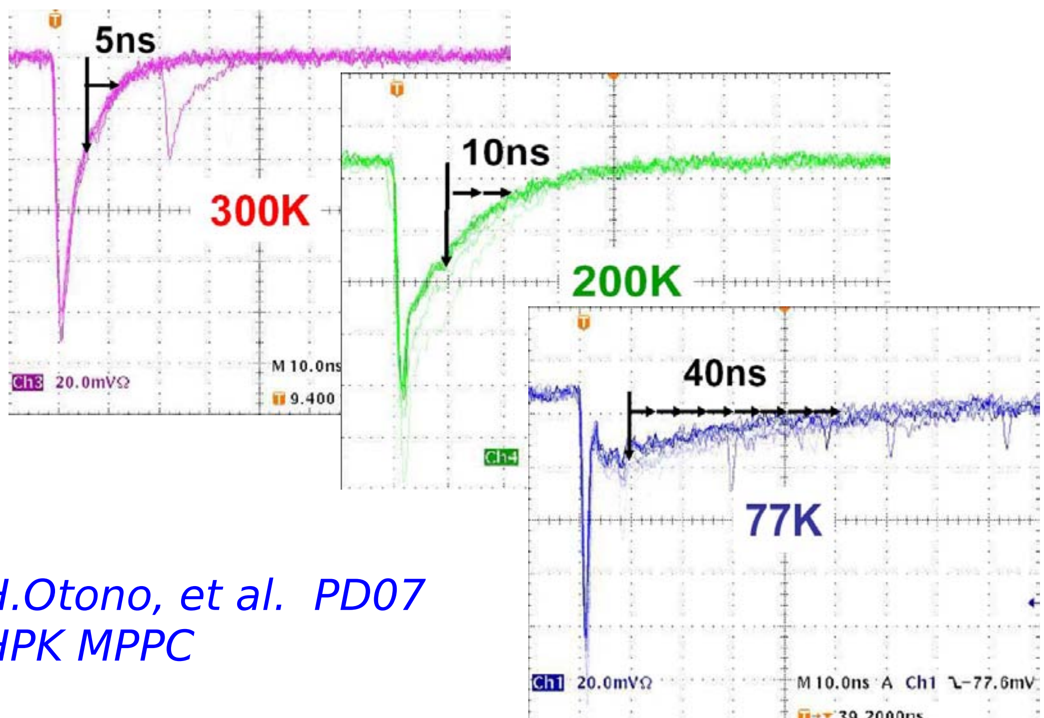

H.Otono, et al. PD07
HPK MPPC

Pulse shape:

The two current components show different behavior with Temperature

→ fast component is independent of T because stray C_q couples to external R_{load}

Overview – SiPM properties at low T

Complete characterization of FBK SIPM in the temperature range 50K<T<320K

1) junction characteristics: forward and reverse (breakdown)
2) gain, dark current, after-pulses, cross-talk
3) photon detection efficiency (PDE)

G.C. et al NIM A628 (2011) 389
and paper in preparation

→ Improved SiPM performances at low temperature (w/ respect to T room):

1) lower dark noise by several orders of magnitude
2) after-pulsing probability constant down to ~100K (then blow up)
3) PDE variations up to ±50% (depending on λ) down to ~100K
4) better timing resolution
5) better $V_{breakdown}$ stability against variations of T

→ SiPM is an excellent alternative to PMT...
...particularly at low temperature !

Experimental Setup

Vacuum vessel (P < 10^{-3} mbar)

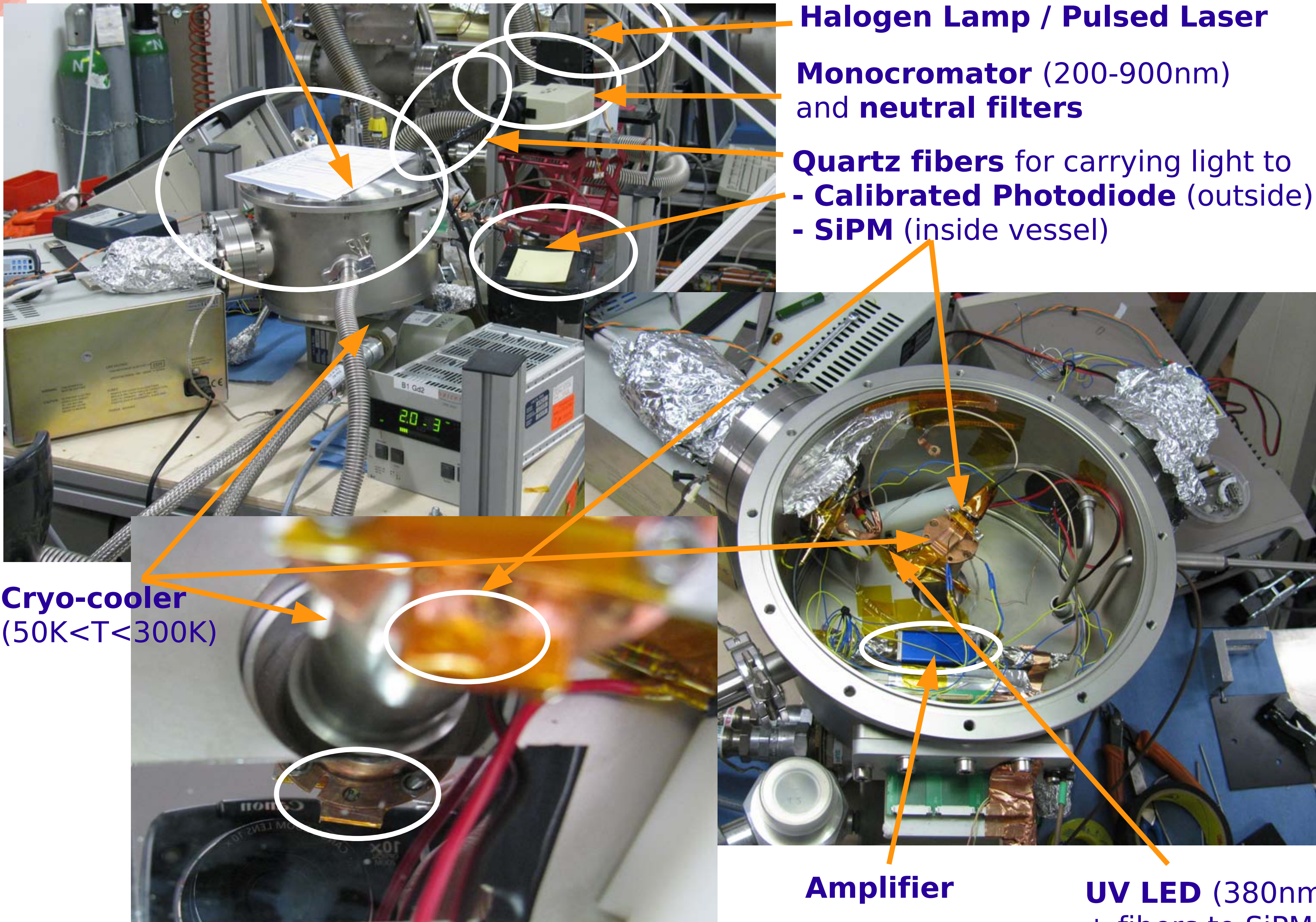

Halogen Lamp / Pulsed Laser

Monocromator (200-900nm) and **neutral filters**

Quartz fibers for carrying light to
- **Calibrated Photodiode** (outside)
- **SiPM** (inside vessel)

Cryo-cooler (50K<T<300K)

Amplifier

UV LED (380nm) + fibers to SiPM

Experimental setup

Temperature control/measurement

- Close cycle, two stages, He cryo-cooler and heating with low R resistor
- Vacuum well below 10^{-3} mbar
- thermal contact (critical) with cryo-cooler head: SIPM within a copper rod + kapton (electrical insulation)
- T measurement with 3 pt100 probes
- Measurements on SiPM carried after thermalization, ie all probes at the same T
- check junction T with forward characteristic

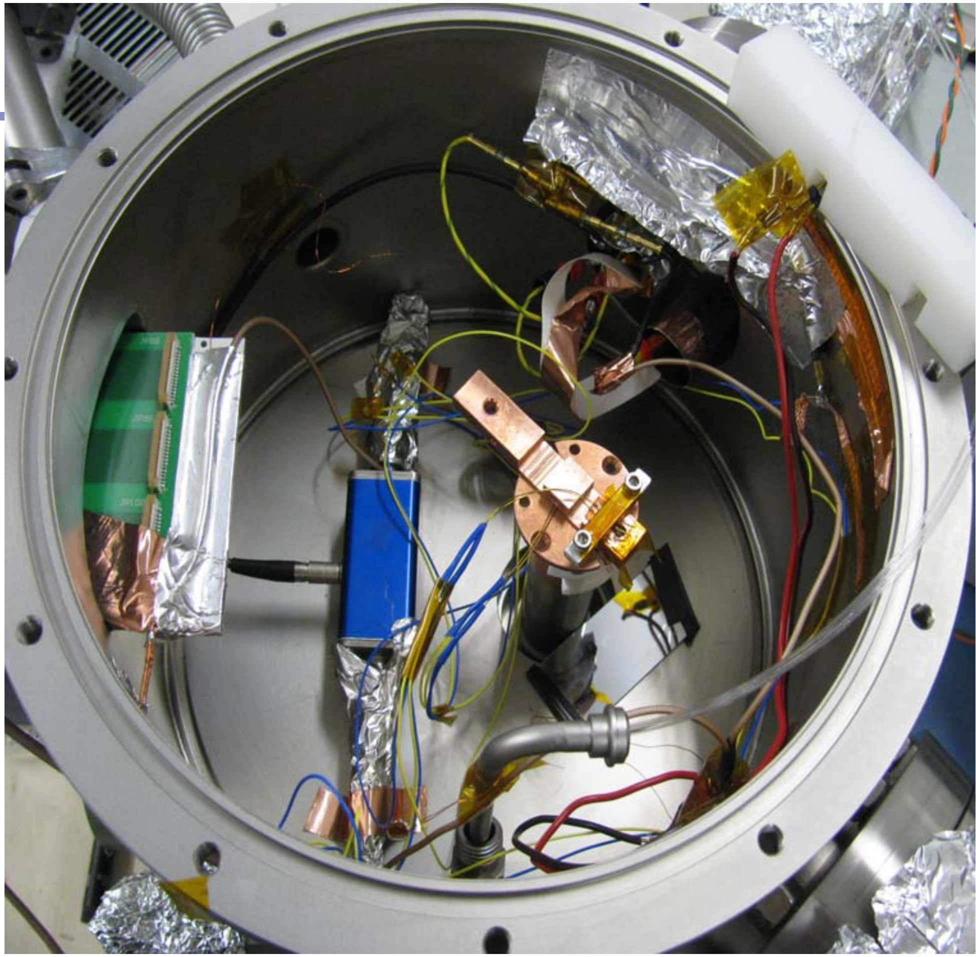

Light sources

- CW: halogen lamp and UV LED (λ~380nm)
- Pulsed: laser (30ps rms, λ~405nm)

V_{bias} and current measurements

- Keytley 2148 Voltage/Current source/meter

Pulse/Waveform sampling

- Care against HF noise → feedthroughs !!!
- Amplifier Photonique/CPTA (gain~30, BW~300MHz)
- Lecroy o.scope, 1GHz, 20GS/s

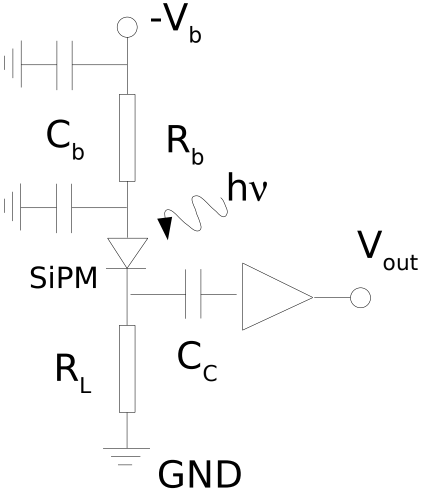

SiPM samples

FBK SiPM (2008) – 1mm^2 (Vbr~33V, fill factor~20%)

- n^+-on-p shallow junction
- 4μm fully depleted region (active volume)
- no protective epoxy (no epoxy cracks at low T)

I-V measurements: forward bias

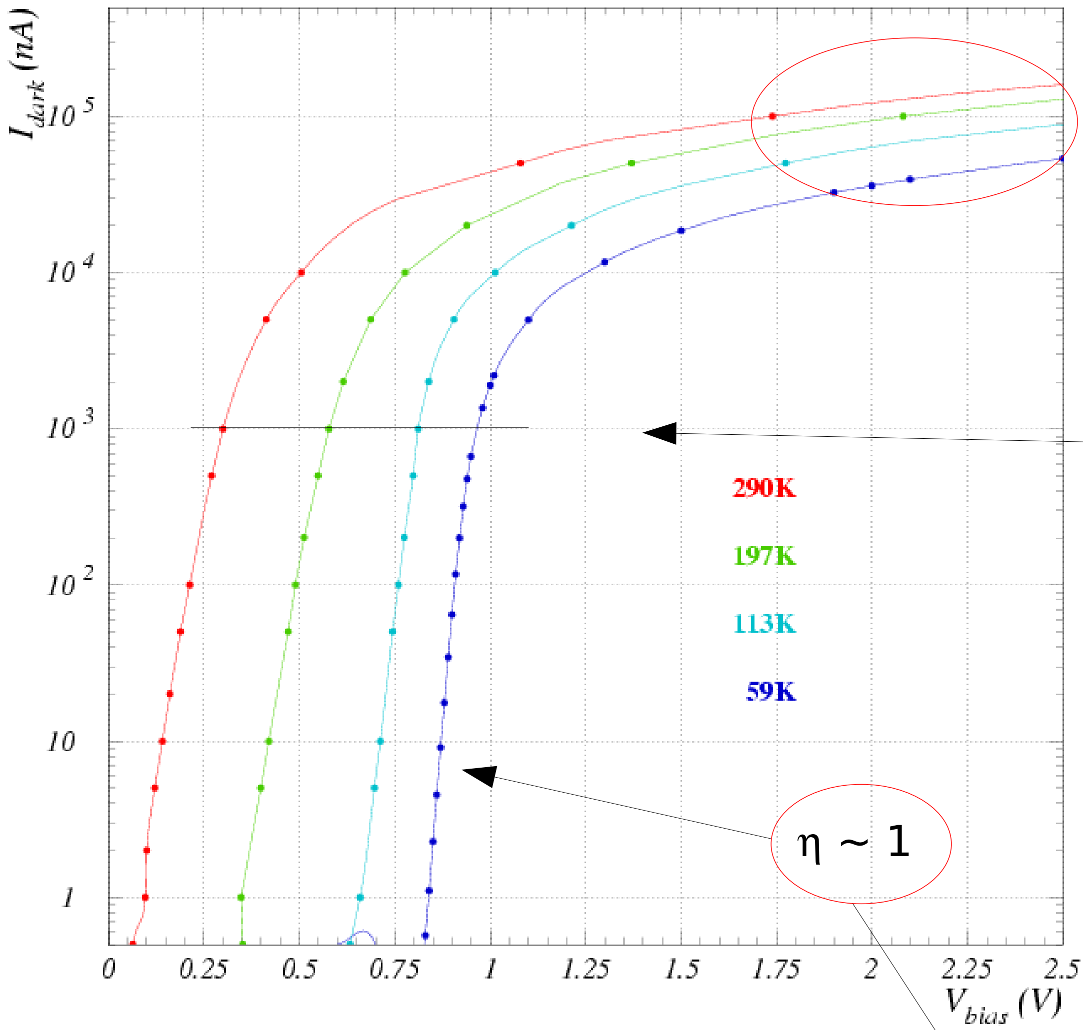

3 **Ohmic** behavior at high current

Linear fit → $R_{series} \sim R_q / N_{cells}$

2 **Voltage drop** (V_d) decreases linearly with T decreasing (e.g. at 1μA)

1 **Forward current**

$$I_{forward} \sim C(\eta) A(T) [\exp(\frac{q V_d}{\eta k T}) - 1]$$

Shockley et al. Proc. IRE 45 (1957)

η ideality factor

Diffusion current dominating: η → 1

Recombination current dominating: η → 2

I-V measurements: forward bias

Voltage drop at fixed forward current → precise **measurement of junction T**...

for T→0 ideally V_d→ Eg
(freeze-out effects apart)

... otherwise not trivially measured !

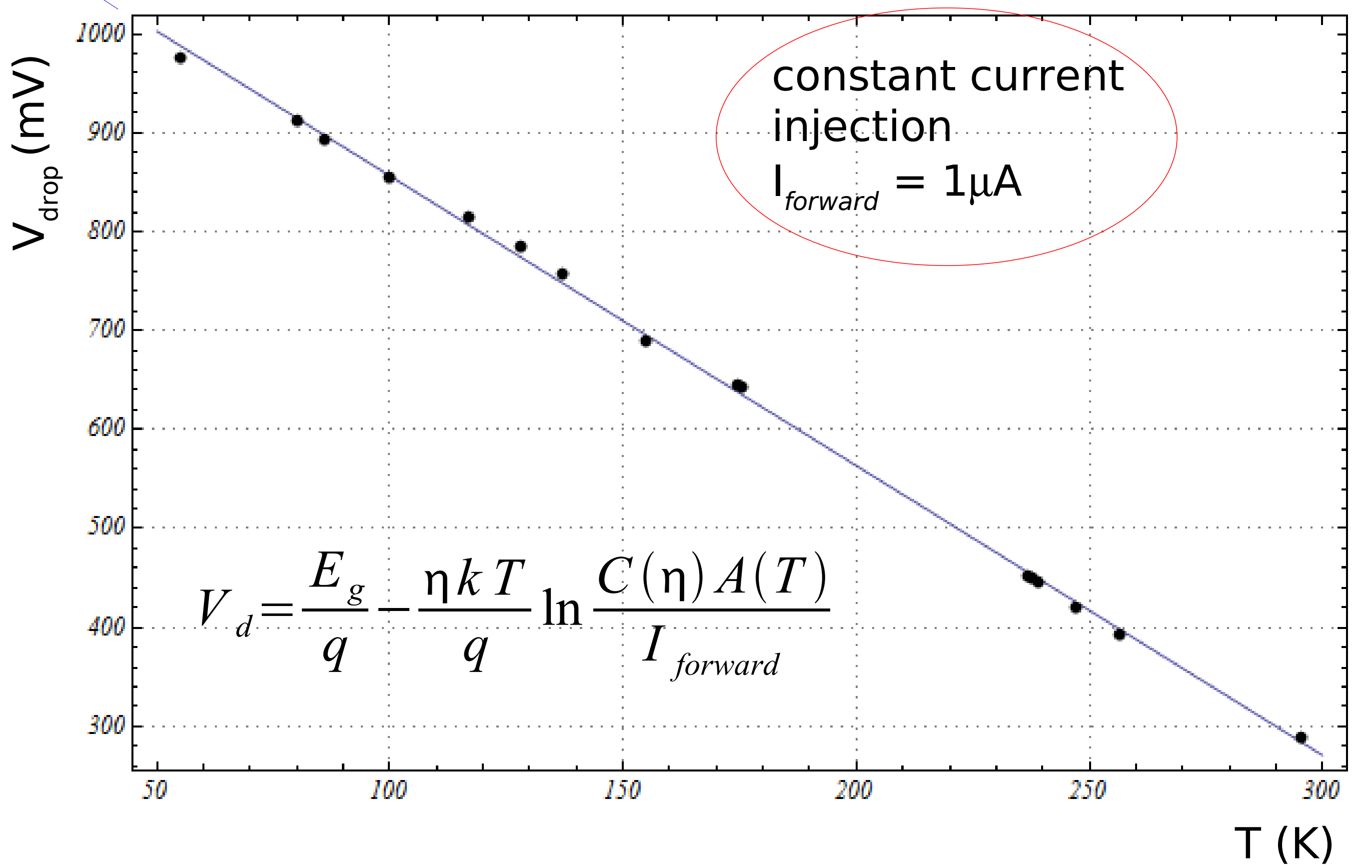

- (almost) linear dependence with slope $dV_{drop}/dT|_{1\mu A}$ ~ -3mV/K
  (we don't see freeze-out effects down to 50K)

- direct and precise **calibration/probe** of junction(s) Temperature

Series Resistance vs T

Two ways for measuring series resistance (R_s)

1) Fit at high V of forward characteristic
2) Exponential recovery time (afterpulses envelope)

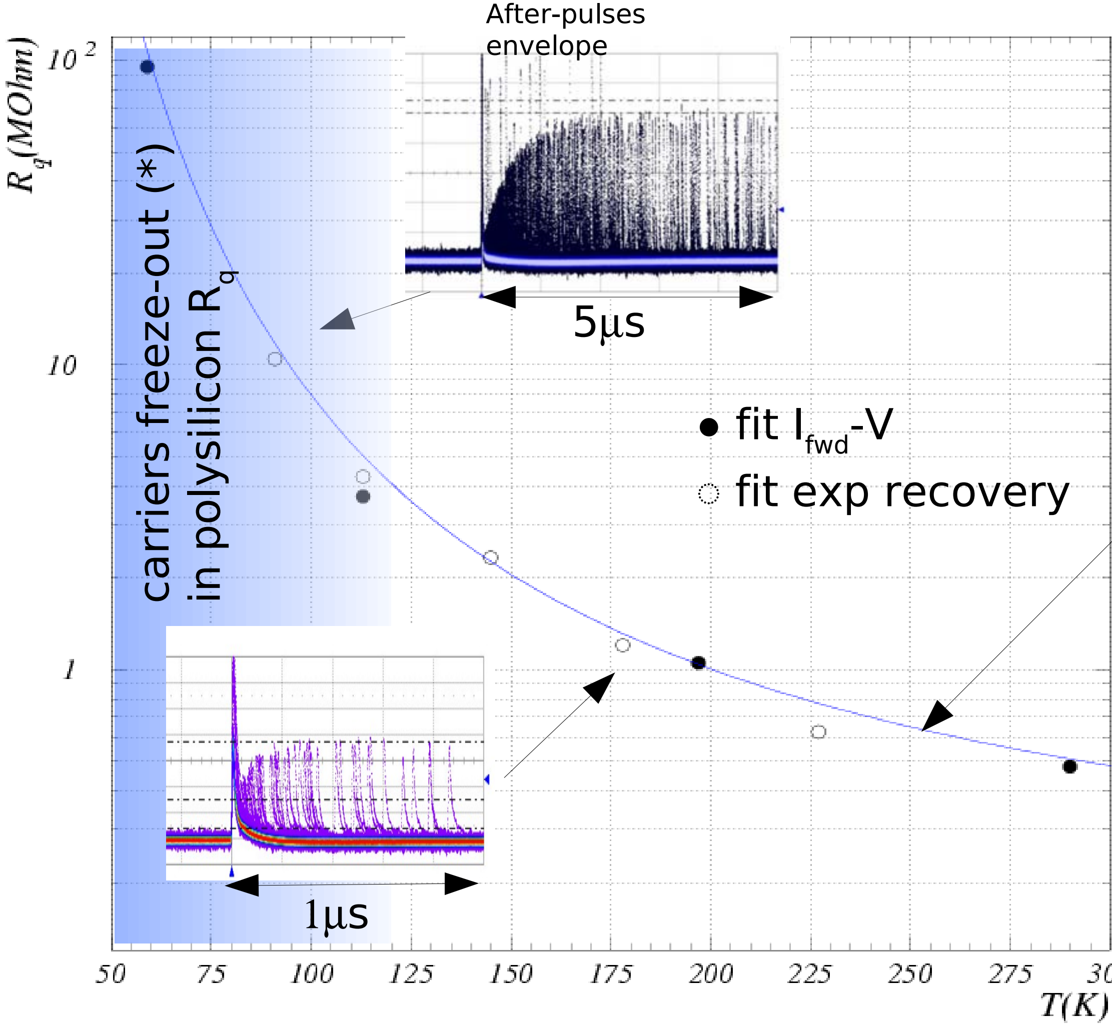

Measurements (1) and (2) consistent → **dominant effect from quenching resistor R_q**
(→ series R bulk gives smaller contribution)

Empirical fit:

$$R_q(T) \sim 0.13\,(1 + 300/T\, e^{300/T})\, M\,\Omega$$

Afterpulses envelope

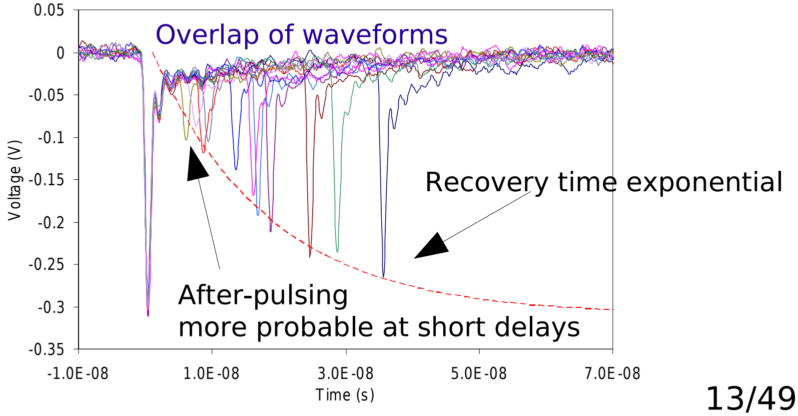

Note: SiPM for low T applications must have appropriate quenching R (not quenching at room T !)

I-V measurements: reverse bias

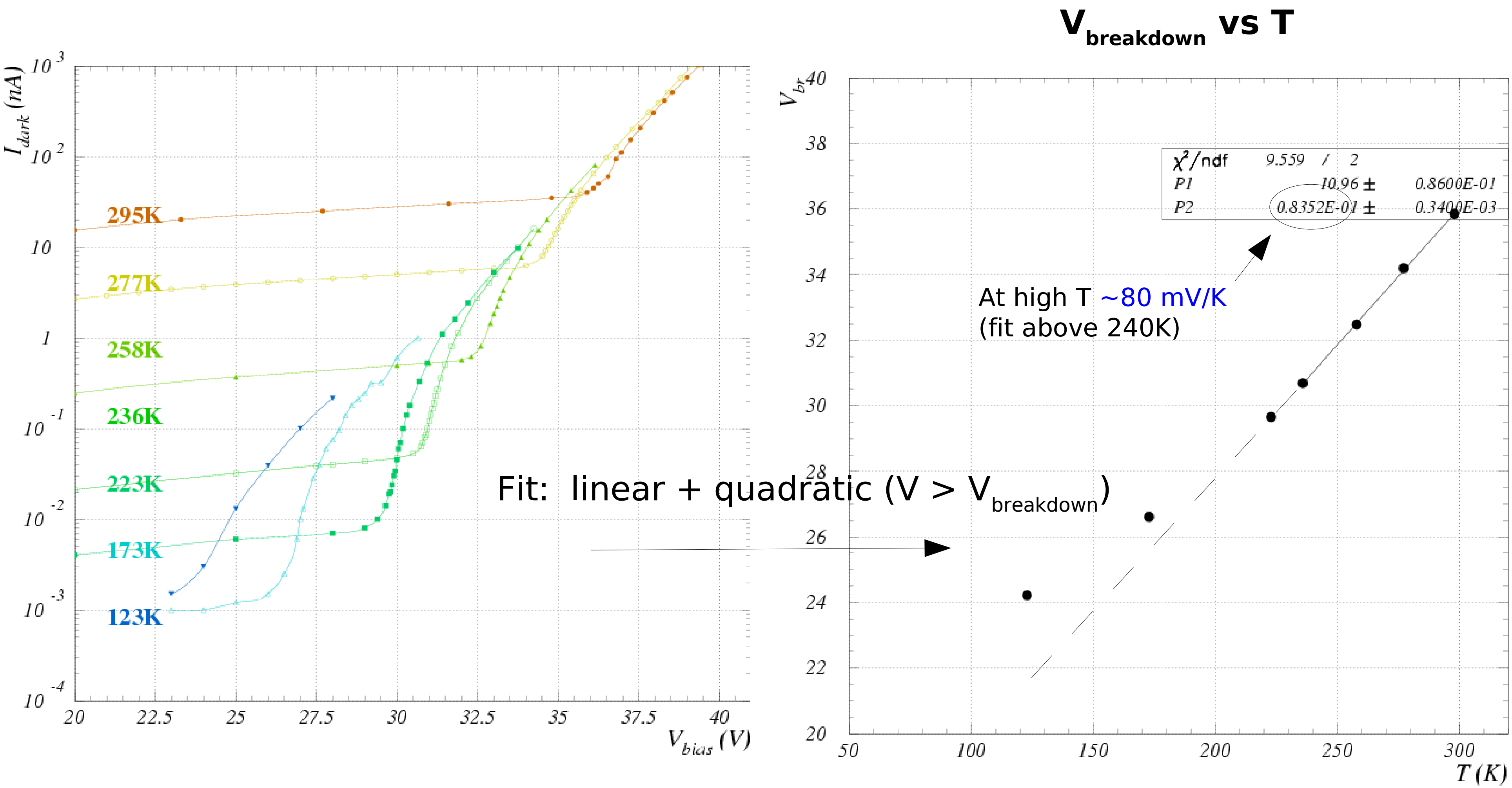

Avalanche breakdown voltage decreases due
to larger carriers mobility at low T → larger ionization rate
(at fixed electric E field)

V breakdown vs T

Breakdown Voltage

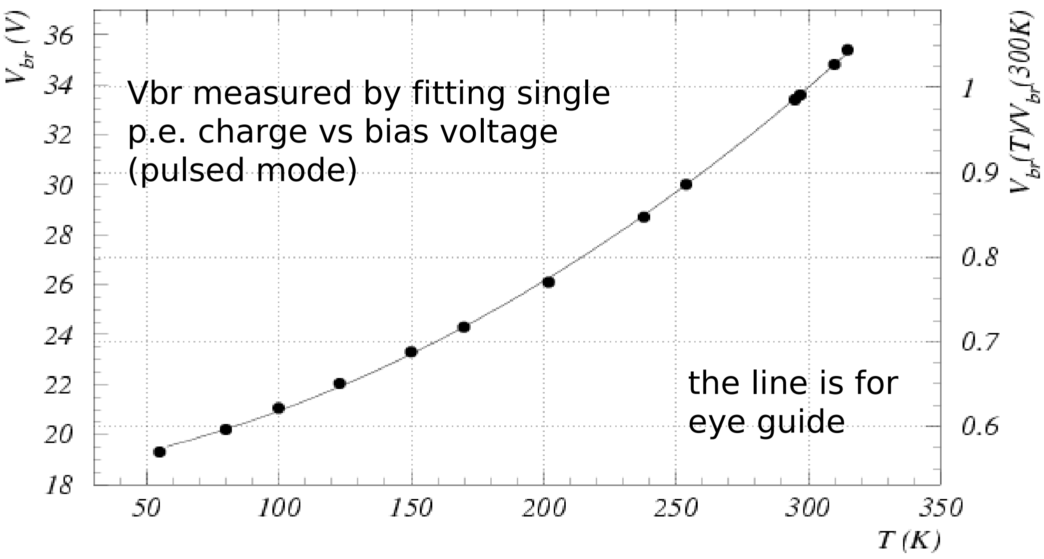

Consistent with Breakdown calculations for abrupt junctions with p-region doping at the level of 10^{17} cm^{-3} (*)

Temperature coefficient

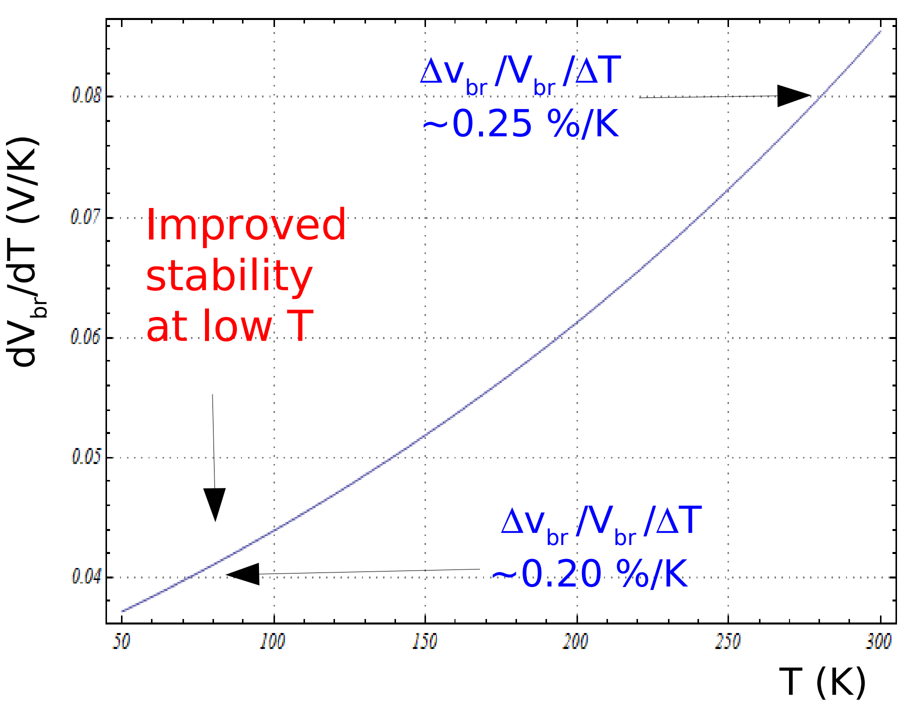

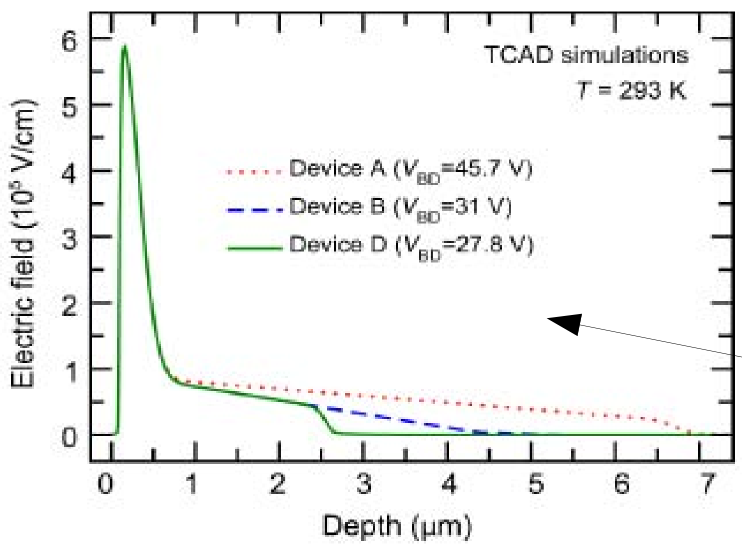

(*) E field profile of FBK SiPMs described in the paper:
Serra et. al. (FBK) "Experimental and TCAD Study of Breakdown Voltage Temperature Behavior in n+/p SiPMs" IEEE TNS 58 (2011) 1233

Dark current vs T (constant ΔV)

(*) the contribution to noise from diffusion of minority carriers is negligible in this T range

Thermal noise mainly due to G-R in the high E Field region (not the whole depletion region)

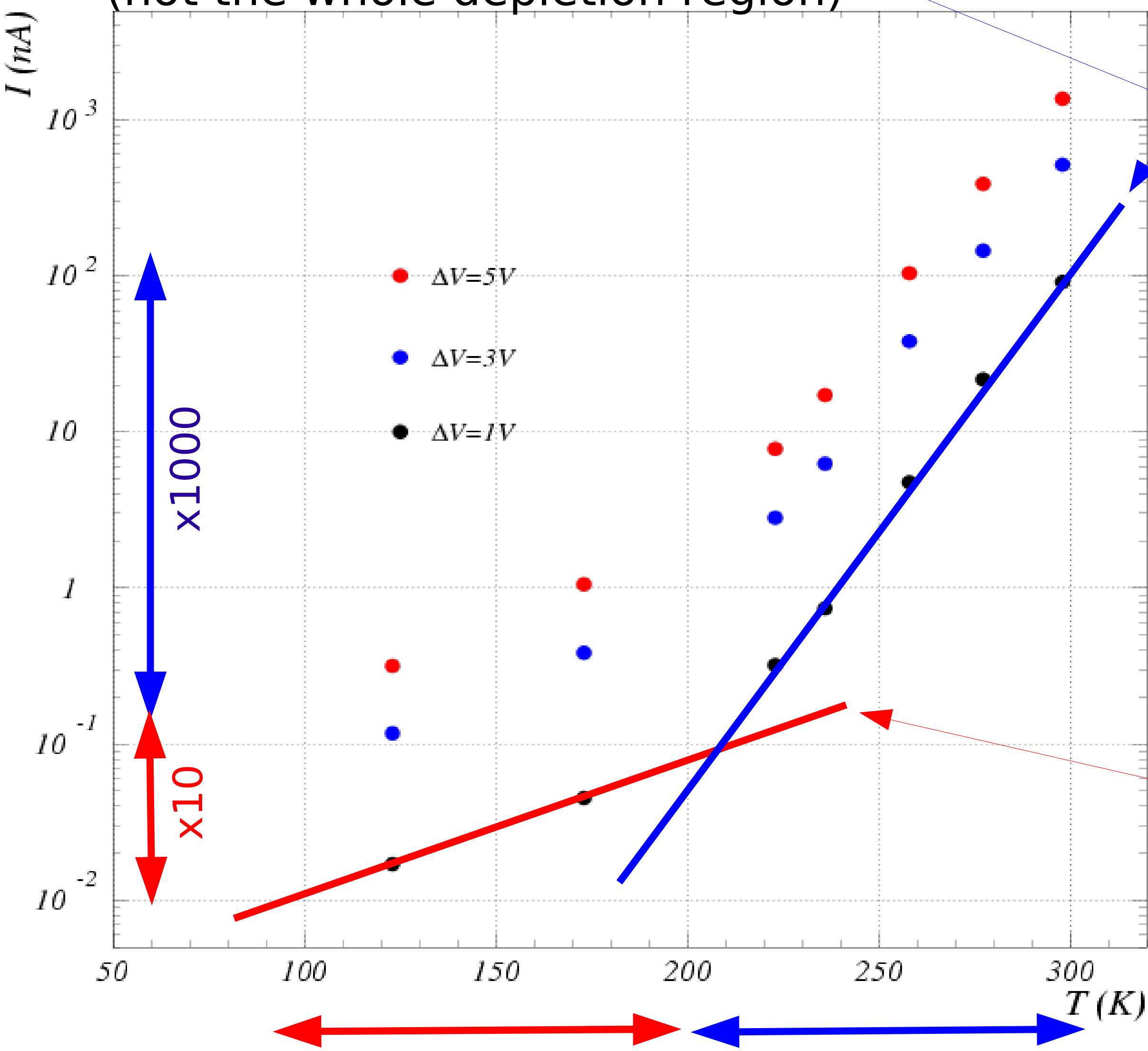

Tunneling noise dominating for T<200K
(FBK devices have E field quite peaked)

Main noise mechanisms (*)

1) Generation/Recombination SRH noise (enhanced by trap assisted tunneling)

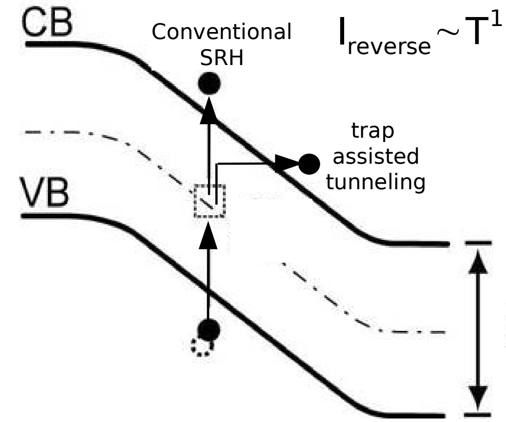

$$I_{reverse} \sim T^{1.5} \exp\frac{-E_{act}}{K_B T}$$

2) Band-to-band Tunneling noise (strong dependence on the Electric field profile)

note: negative T coefficient

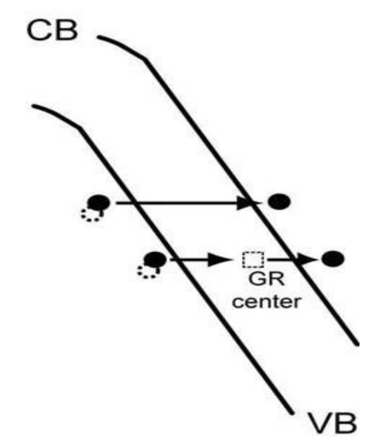

Dark count rate vs T (constant ΔV)

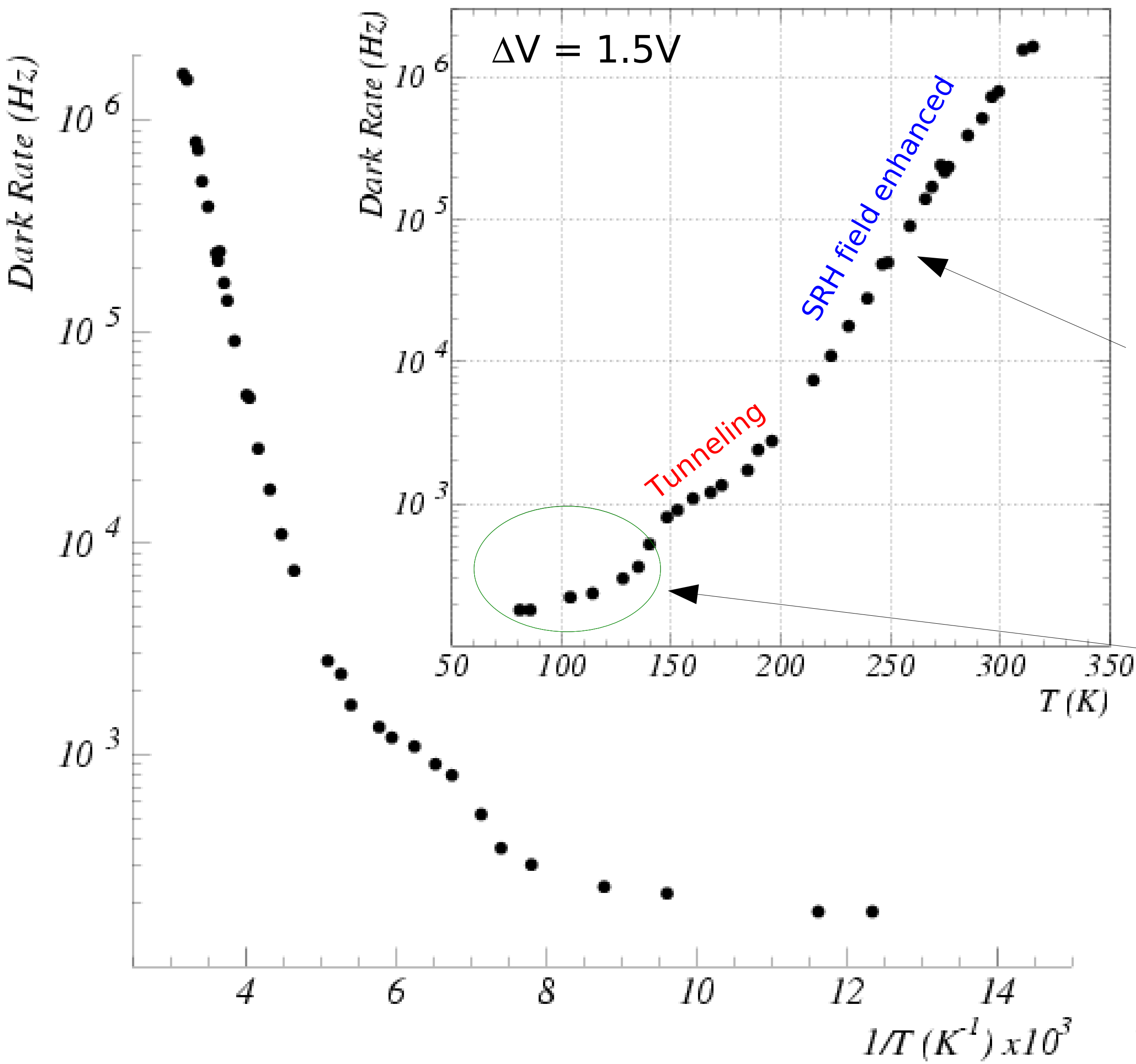

Measurement of
counting rate of ≥1p.e.
at fixed ΔV=1.5V
(→ constant gain)

$$DCR \sim T^{1.5} \exp \frac{-E_{act}}{2K_B T}$$

Activation energy E_{act}~0.72eV

Note: E_{act} should be ~ E_g but tunnelling makes effective gap smaller

? Additional structure
? carriers freeze-out (*)

(*) carrier losses at very low T due to ionized impurities acting as shallow traps

After-Pulsing

Carrier trapping and delayed release

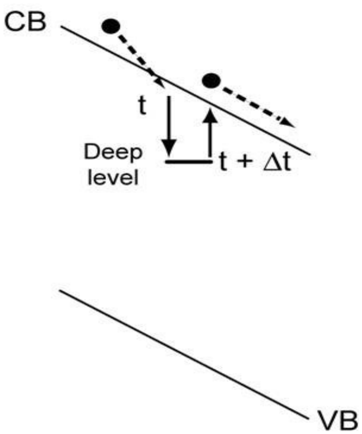

$$P_{afterpulsing}(t) = P_c \cdot \frac{\exp(-t/\tau)}{\tau} \cdot P_{trigg} \propto \Delta V^2$$

~Few % level at 300K

avalanche triggering probability
$\propto \Delta V(t)$

τ : trap lifetime
depends on trap level position

quadratic dependence on ΔV

P_c : trap capture probability
$\propto$ carrier flux (current) during avalanche $\propto \Delta V$
$\propto$ N traps

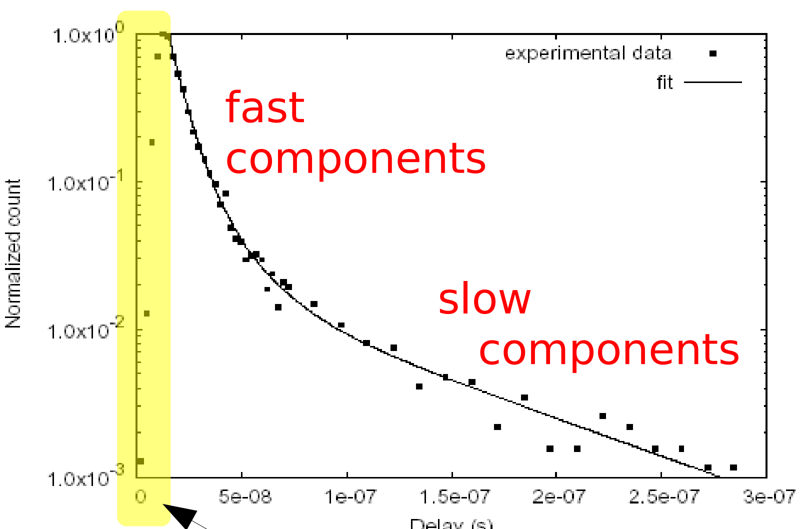

Fig. 10. Spectrum of the delay time from the primary pulse to the after-pulse.

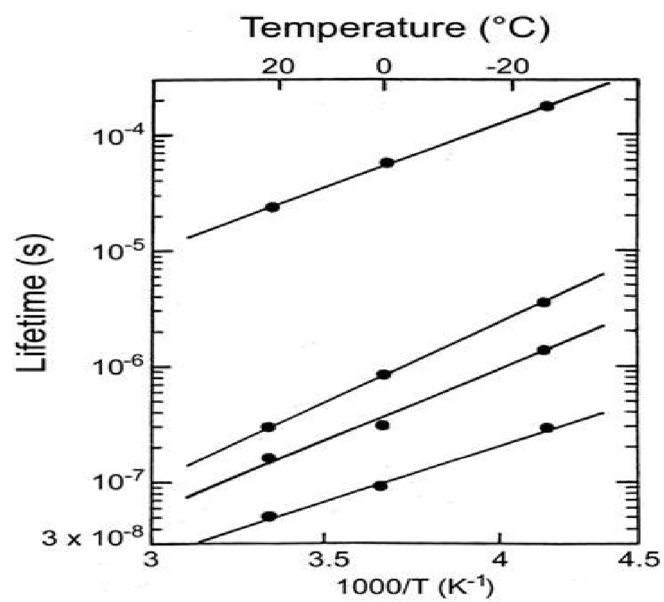

S.Cova, A.Lacaita, G.Ripamonti, IEEE EDL (1991)

Partially sensitive to after-pulsing during recovery

After-Pulses vs T (constant ΔV)

Measurement by waveform analysis:
- trigger on single carrier pulses (with no preceding pulses within Δt=5μs), **count subsequent pulses** within Δt=5μs (find the after-pulsing rate r_{AP})
- Subtract dark count contribution
- extract **after-pulsing probability P_{AP}** corrected for after-pulsing cascade

$$P_{AP} = \frac{r_{AP}}{1 + r_{AP}}$$

ΔV = 1.5V

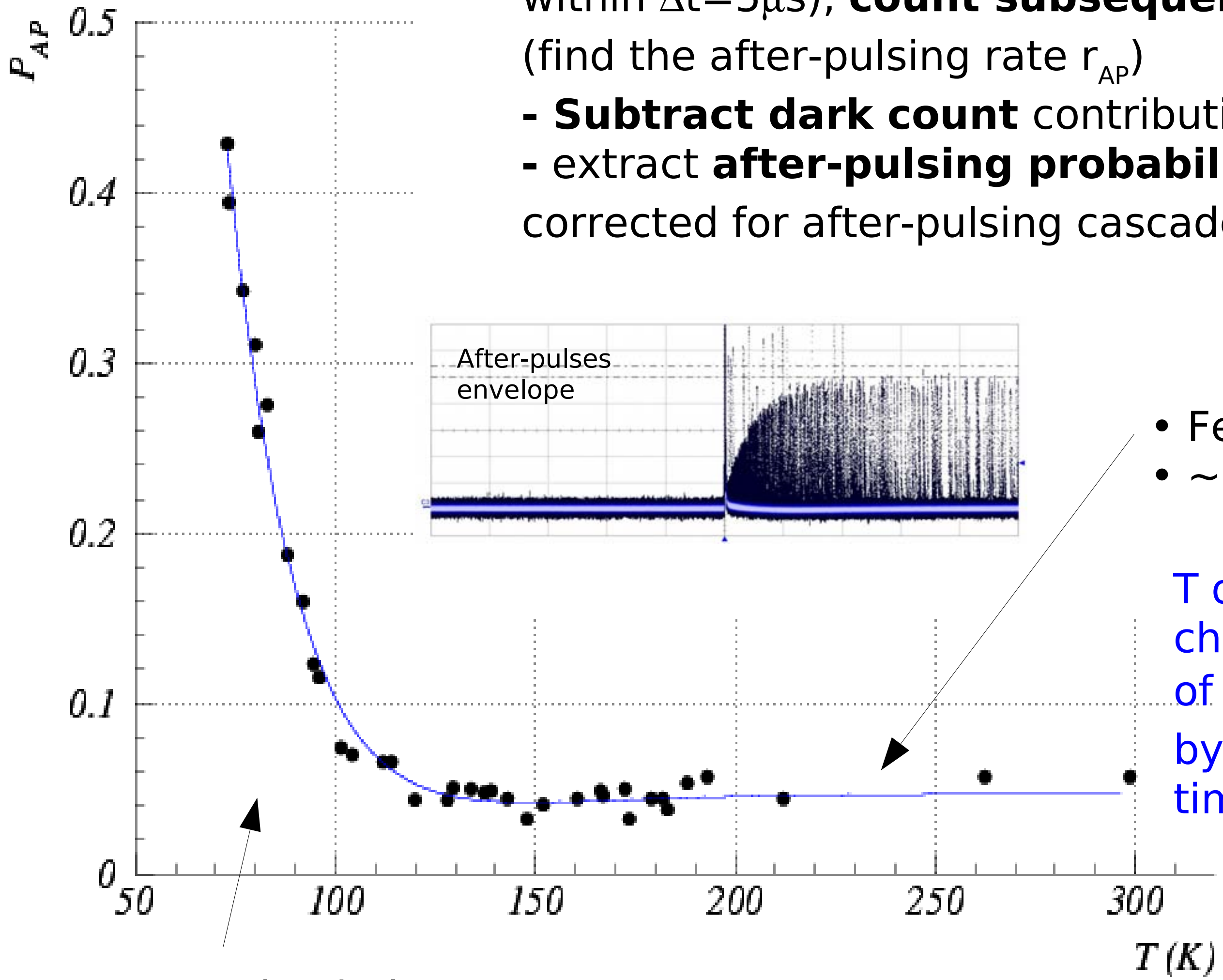

- Few % at room T
- ~constant down to ~120K

T decreasing: ? increase of characteristic time constants of traps (τ_{traps}) is compensated by increasing cell recovery time (R_q)

- several % below 100K

T<100K: additional trapping centers activated ? possibly related to onset of carriers freeze-out [under investigation]

→ Analysis of life-time evolution vs T of the various traps (at least 3 types at T_{room}) [under investigation]

DR, AP, Gain, X-talk vs ΔV (constant T)

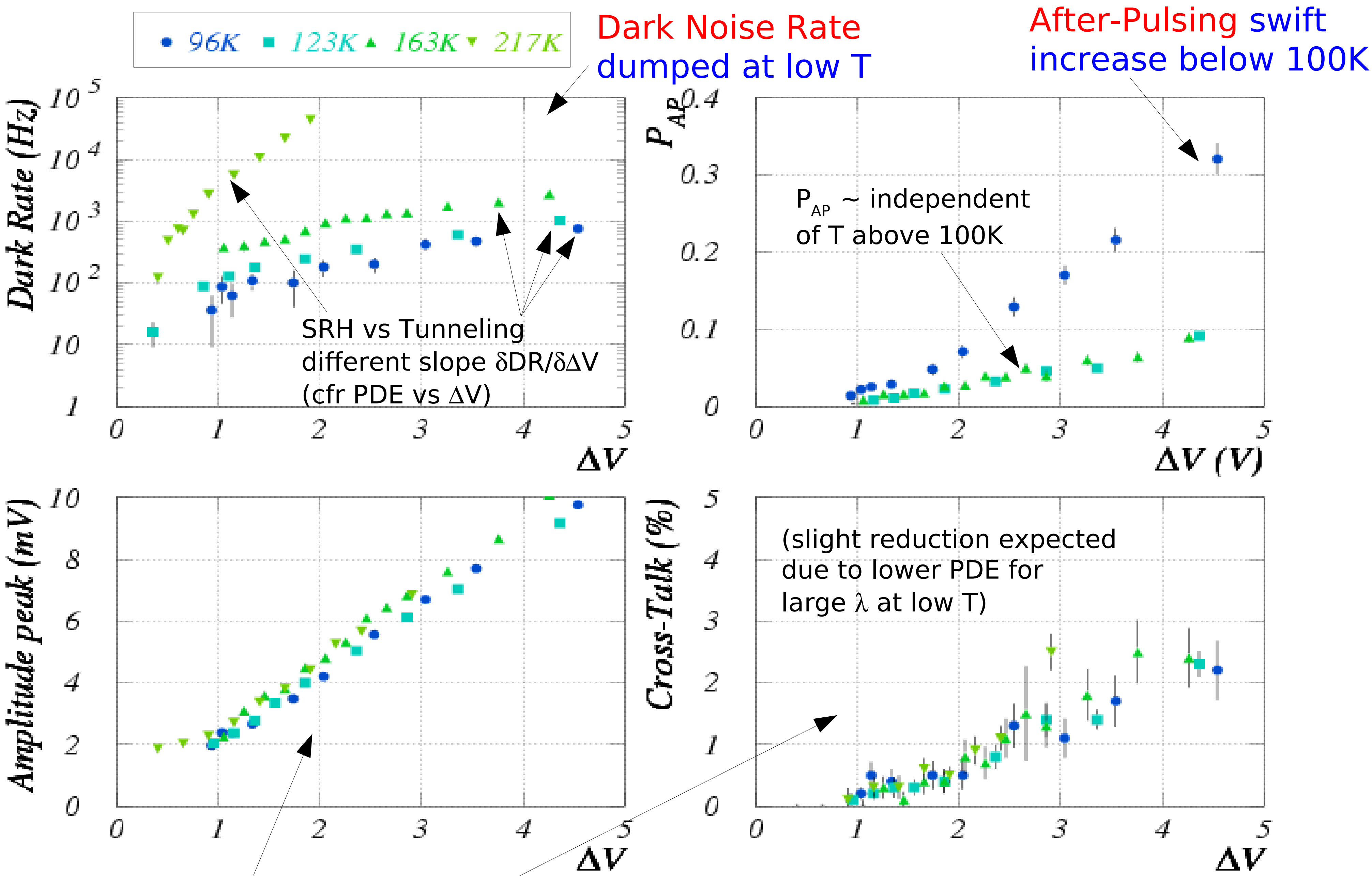

Gain and Cross-Talk are independent of T

Photo-Detection Efficiency (PDE) vs ΔV and λ

SiPM with ε_{geom} ~22%

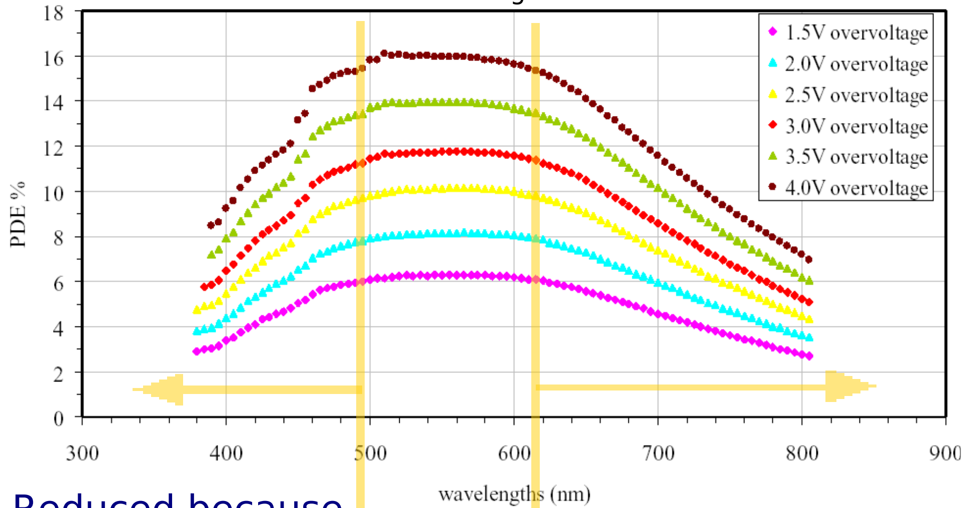

Reduced because avalanche triggered by holes (and ARC)

Reduced because low QE

PDE dependence on λ
(at different ΔV) – room T

PDE =

ε_{geom} (fraction of active area)

x

Transmission efficiency

x

QE (efficiency of photo-conversion) (*)

x

P_{trigg} (avalanche triggering probability)

Expected to be T dependent

(*) factor (1-Probability of recombination) should also be included

SiPM with ε_{geom} ~50%

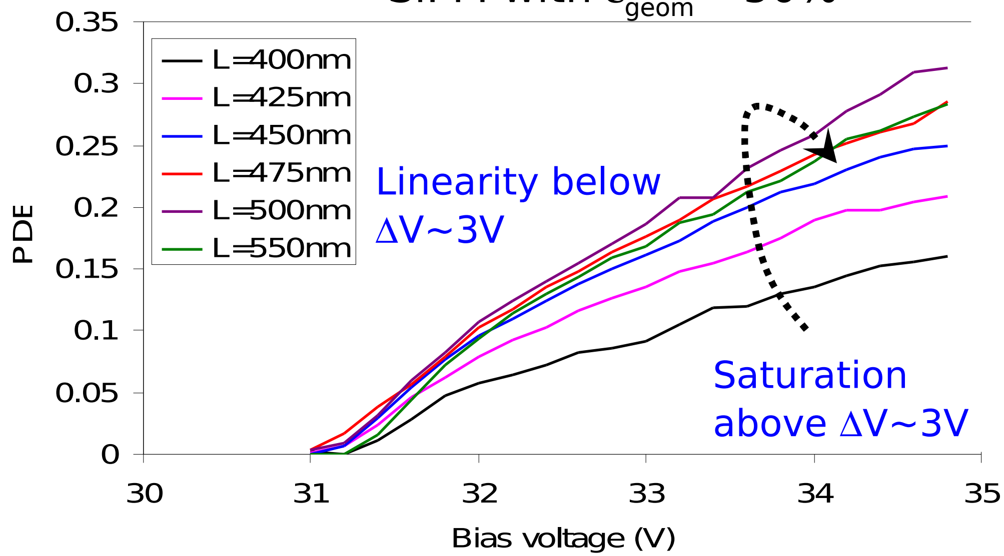

PDE dependence on ΔV
(at different λ) – room T

PDE vs λ (constant ΔV=2V) - halogen lamp (CW)

Measure →
- I_{sipm} / G = current drawn by SiPM / SiPM Gain
- $I_{photons}$ = rate of photons by calibrated photo-diode

→ Find: $\boldsymbol{PDE_{a.u.} = I_{sipm} / G / I_{photons}}$

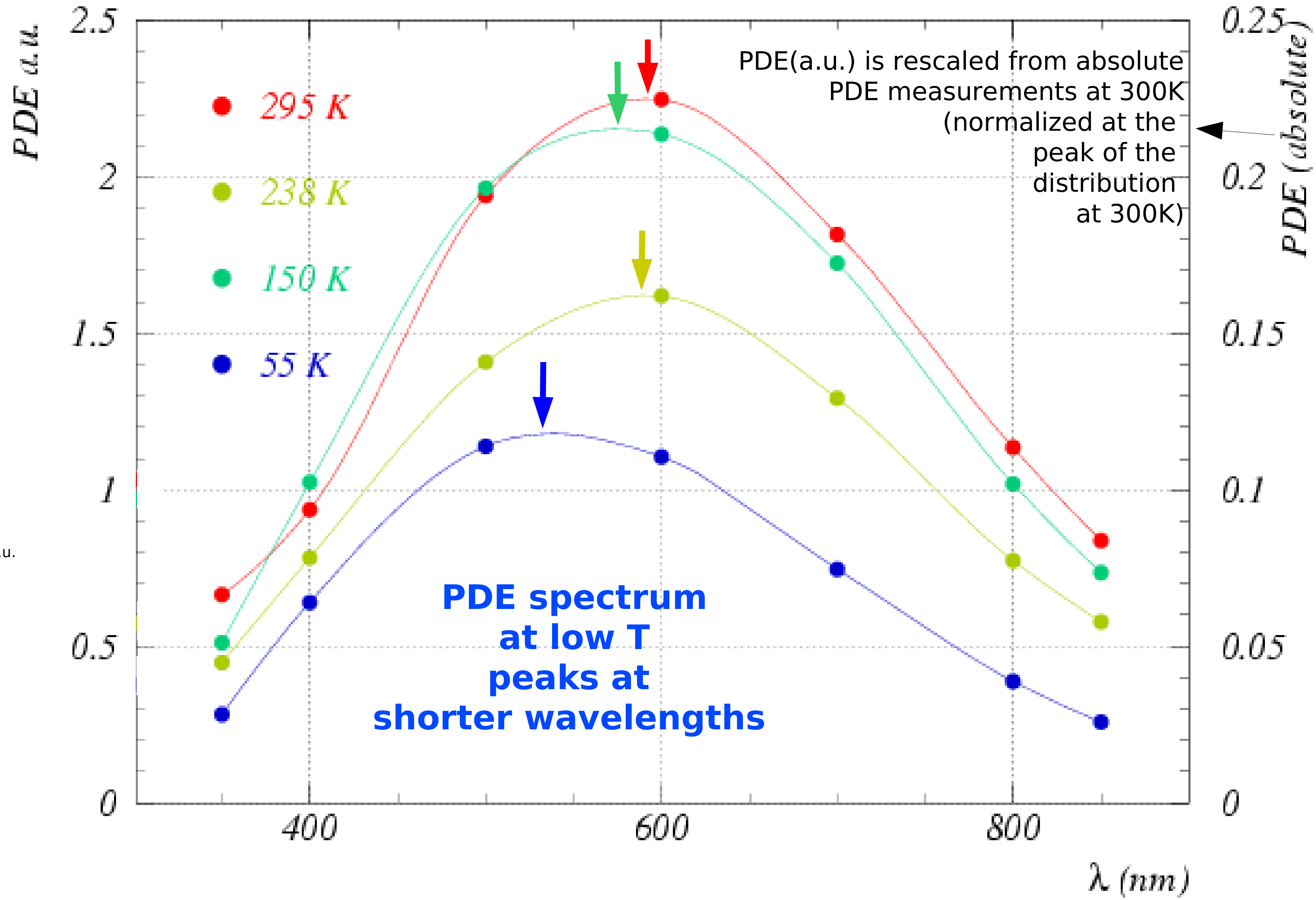

The measured PDE $_{a.u.}$ differs from the absolute PDE by a single normalization factor due to a different photon acceptance of SiPM wrt calibrated diode (different light paths)

PDE vs T (constant ΔV=2V) - halogen lamp (CW)

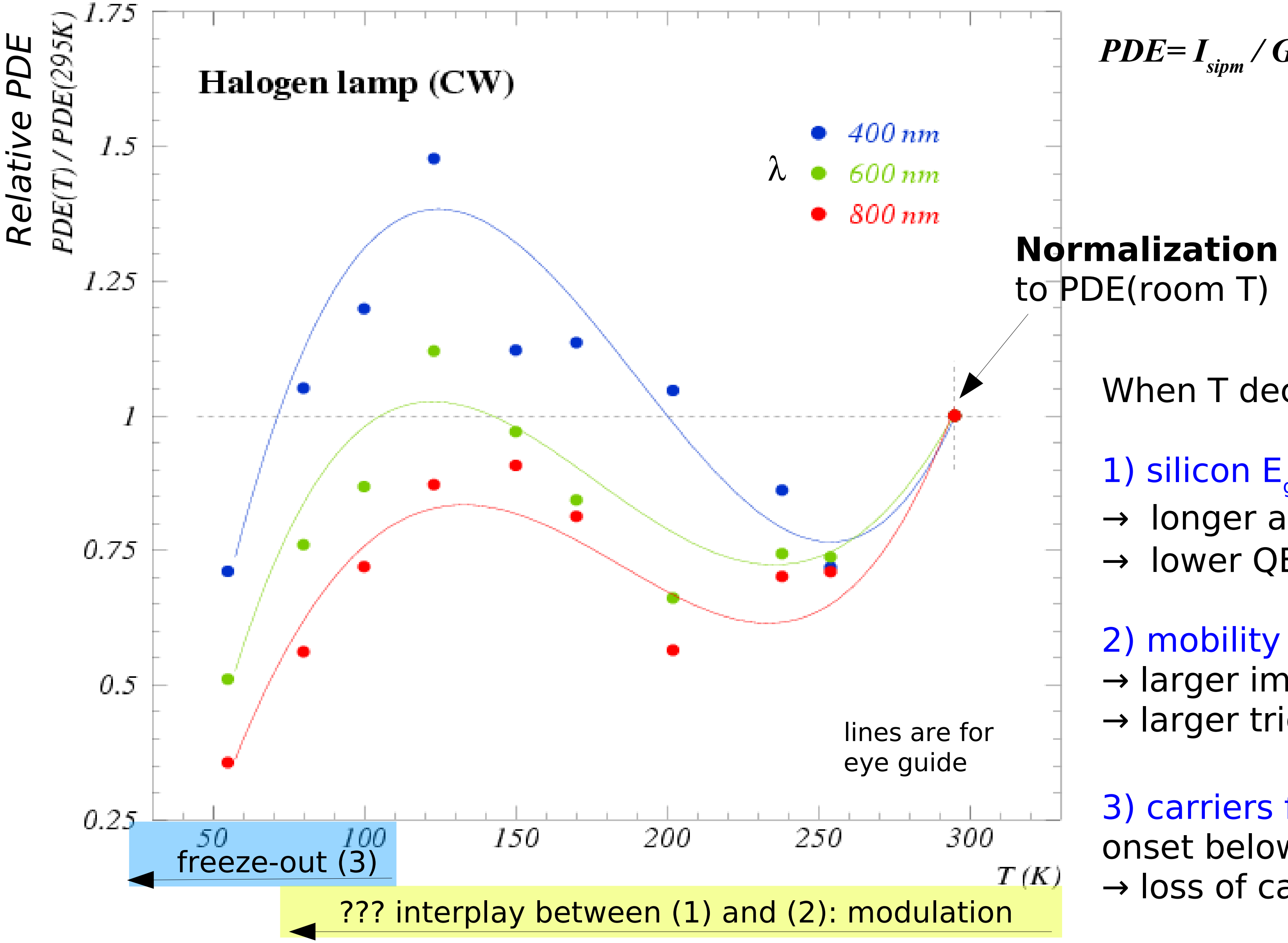

$PDE = I_{sipm} / G / I_{photons}$

When T decreases we expect:

1) silicon E_{gap} increasing
→ longer attenuation length
→ lower QE (for longer λ)

2) mobility increasing
→ larger impact ionization
→ larger trigg. avalanche P_{01}

3) carriers freeze-out
onset below 120K
→ loss of carriers

PDE vs T (ΔV=2V) – LED (CW) and Laser (pulsed)

PDE dependence on T at constant gain:
similar results with LED (cont. light - 380nm) and Laser (pulsed light – 405nm)

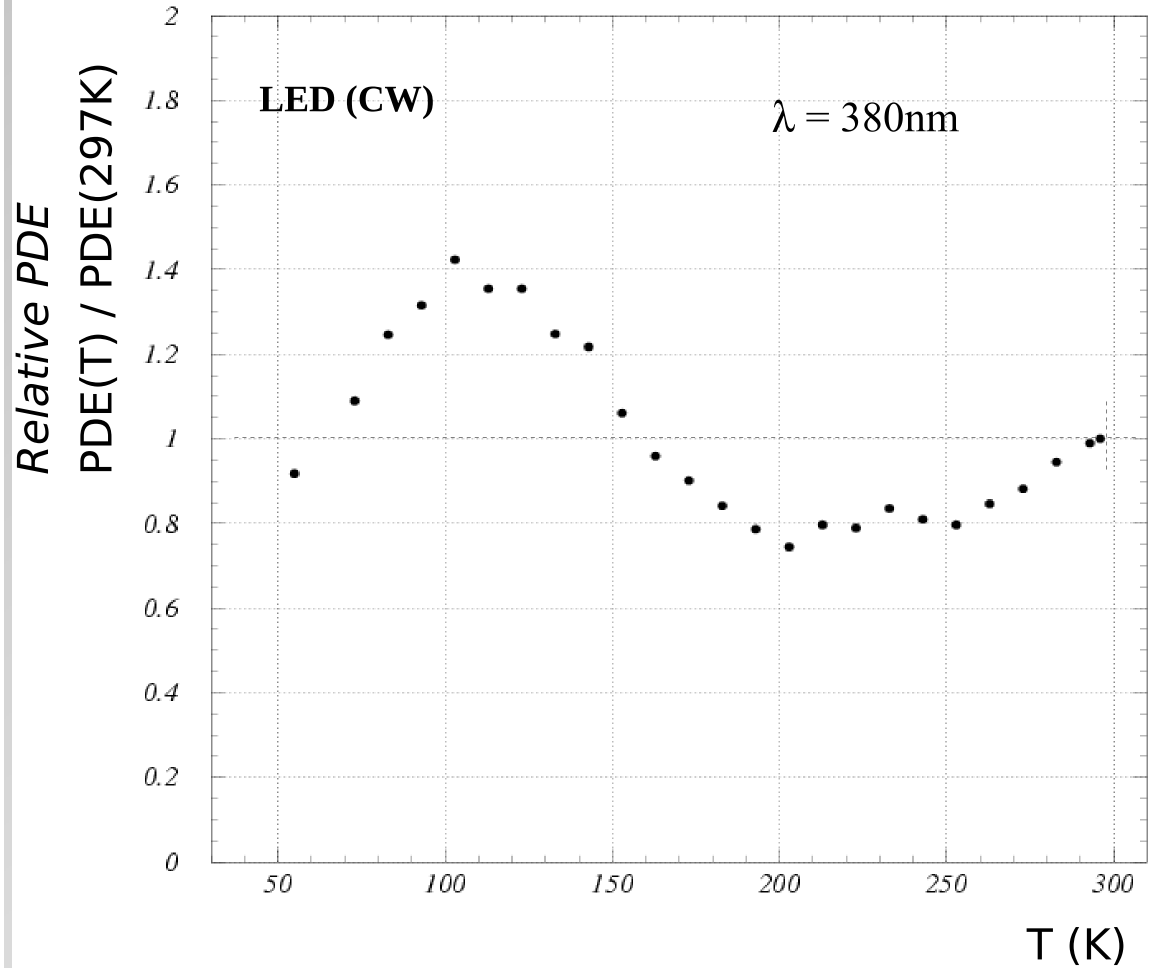

$PDE\,(T) \equiv I_{SiPM}\,(T)\,/\,I_{LED}$

Normalization with PDE at T=297K

Some features similar to APDs (sub-geiger mode)

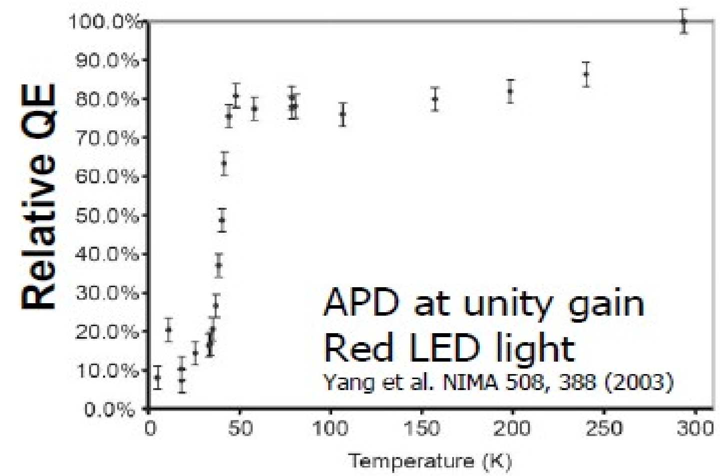

APD at 400nm < λ < 700nm
Johnson et al, IEEE NSS 2009

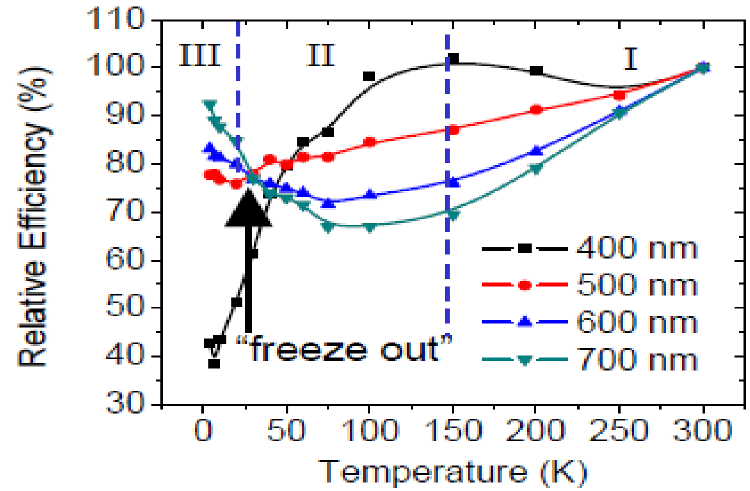

Additional effects in APD (depletion region depends on T, ...)

PDE vs ΔV (constant T) – pulsed laser (405nm)

Measure →

- I_{pe} = average number of p.e. in coincidence with laser trigger x trigger rate
- $I_{photons}$ = average rate of photons measured by calibrated photo-diode

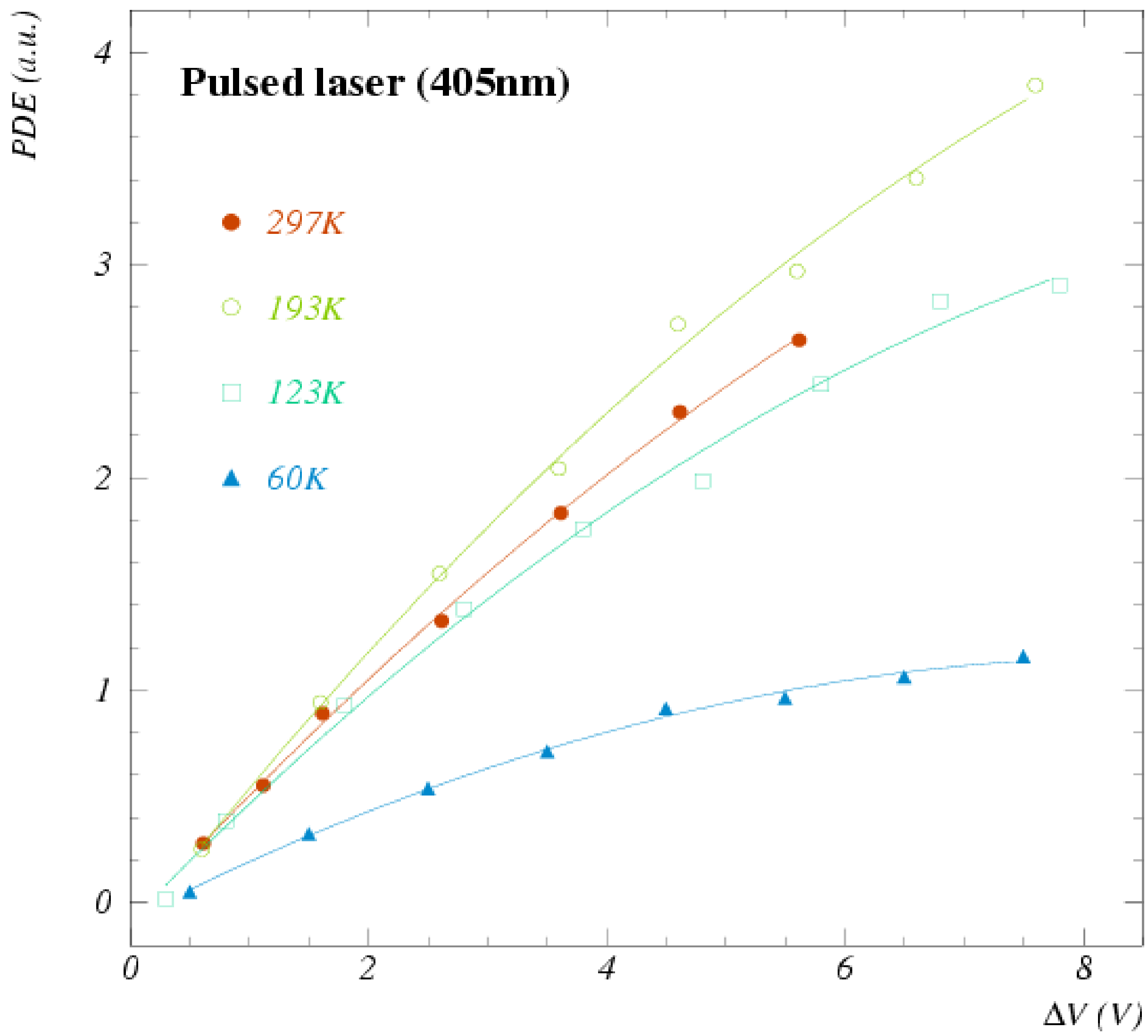

→ Find: $PDE = I_{pe} / I_{photons}$

The measured PDE $_{a.u.}$ differs from the absolute PDE by a single normalization factor due to a different photon acceptance of SiPM wrt calibrated diode (different light paths)

Saturation starts earlier at low T

Understanding PDE vs T

Doping and Field profiles (FBK)

Serra et al (FBK) IEEE TNS 58 (2011) 1233

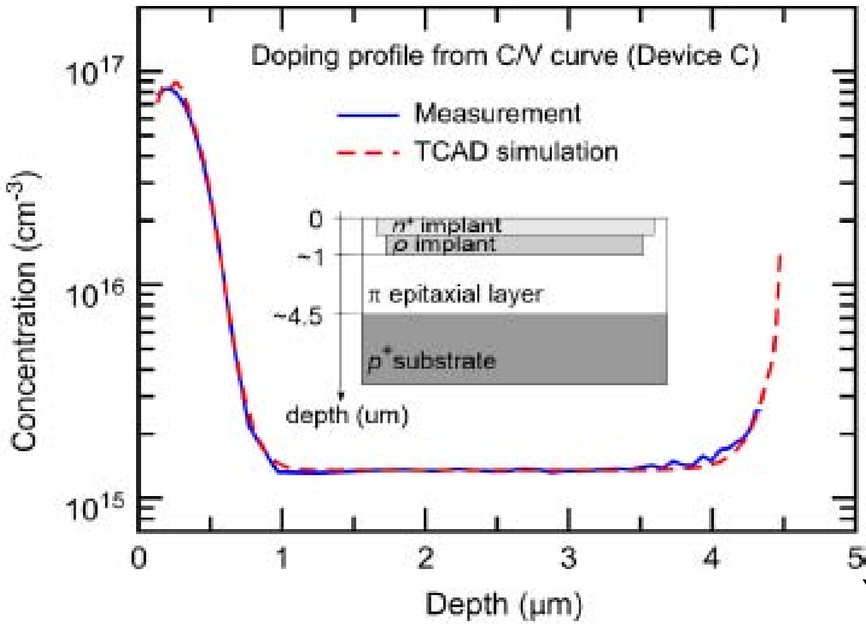

Light absorption in Silicon

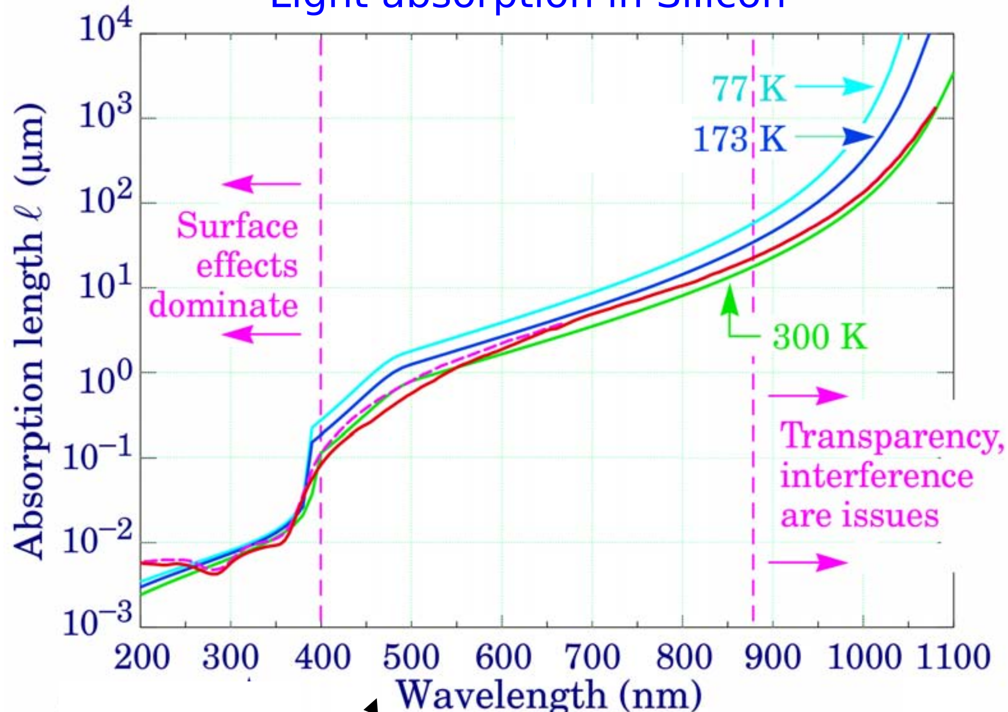

V_{BD} versus doping concentration

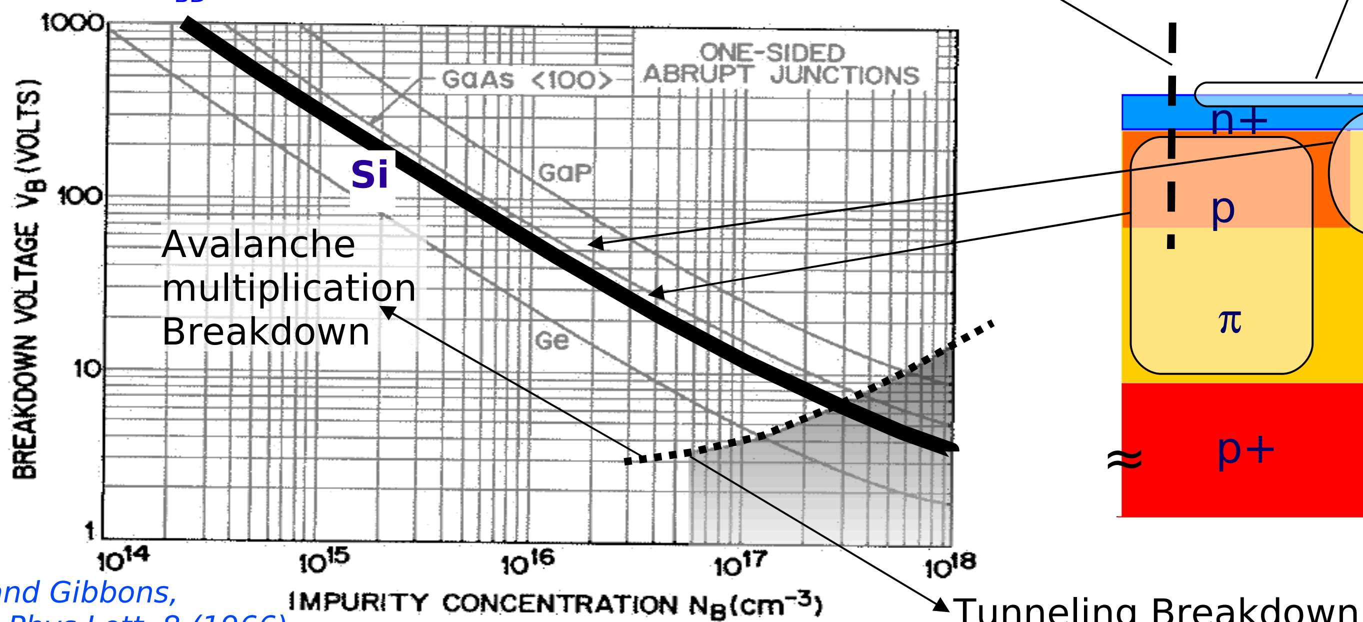

Sze and Gibbons, Appl. Phys Lett. 8 (1966)

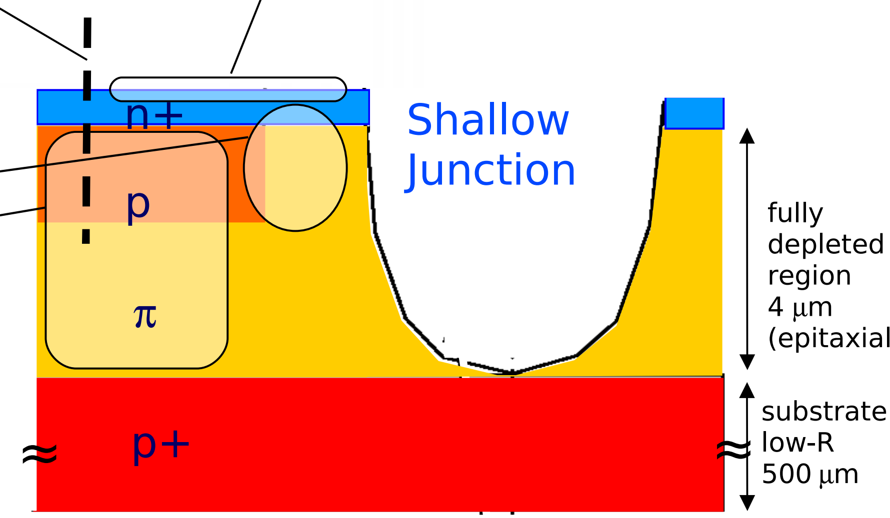

Understanding PDE vs T: 1D toy model

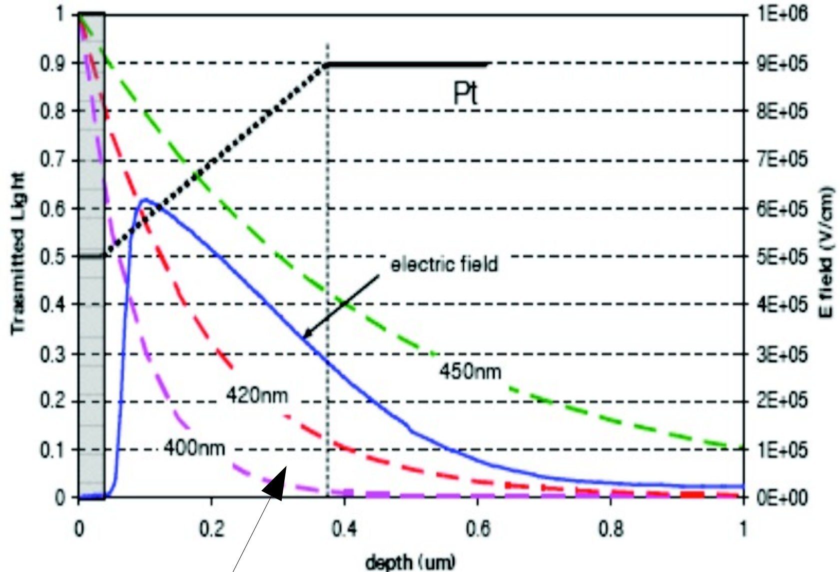

E field profile +

+ impact ionization rate

calculate

Breakdown voltage vs T

Avalanche triggering probability
for electrons and holes ($P_{trigger}e$, $P_{trigger}h$)
(using differential equations method after *Oldham et al, IEEE TNS 19 (1972) 1056)*

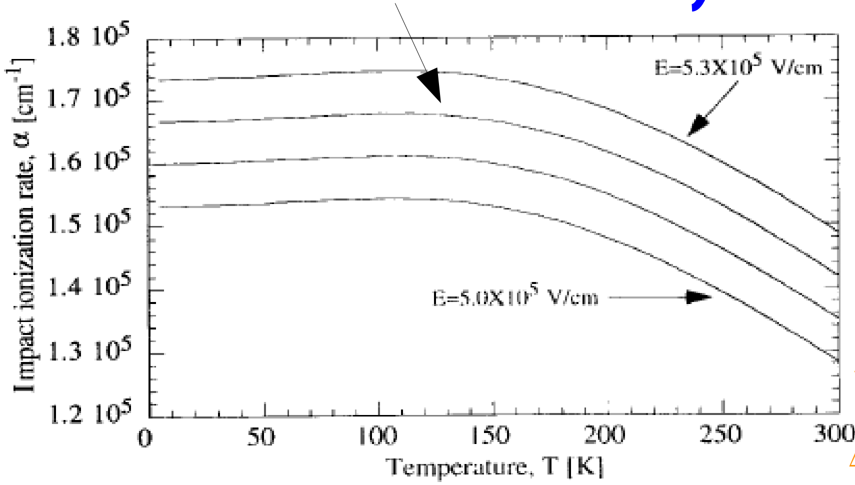

FIGURE 1.43. The impact ionization rate α as a function of temperature T_A with the electric field E as a parameter calculated from Okuto and Crowell's (85) model.

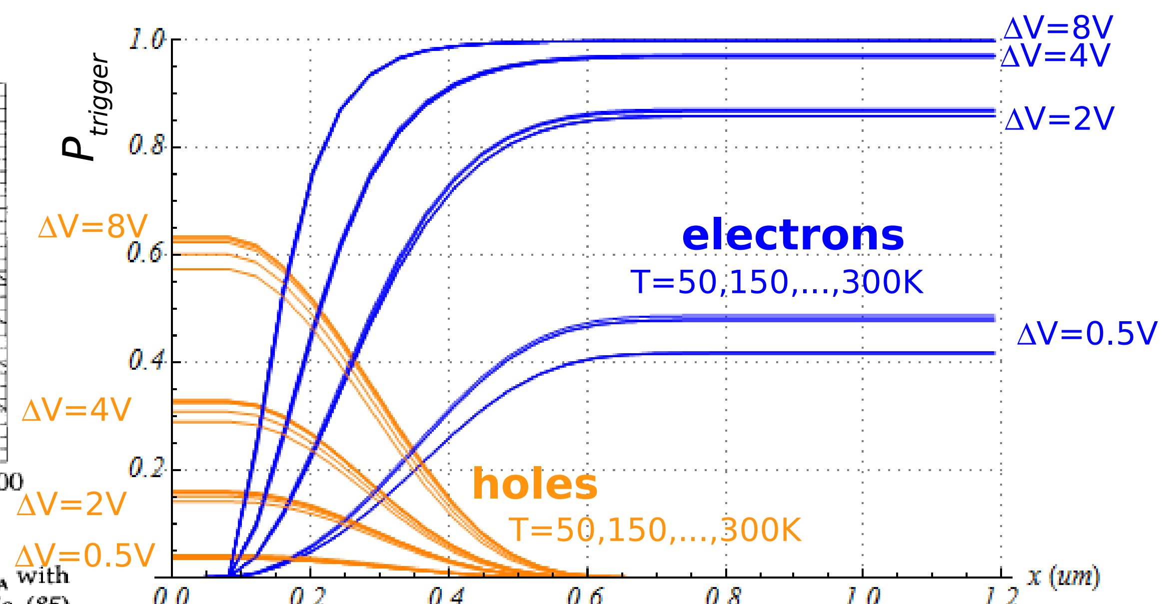

Understanding PDE vs T: 1D toy model

avalanche triggering probability +

\+ light **absorption length in Si (1/α)**

calculate → **PDE as a function of (λ ,T,ΔV)** obtained by the convolution of $P_{trigg}(x)$ and $\alpha \exp(-\alpha x)$ (integrated over the depletion layer)

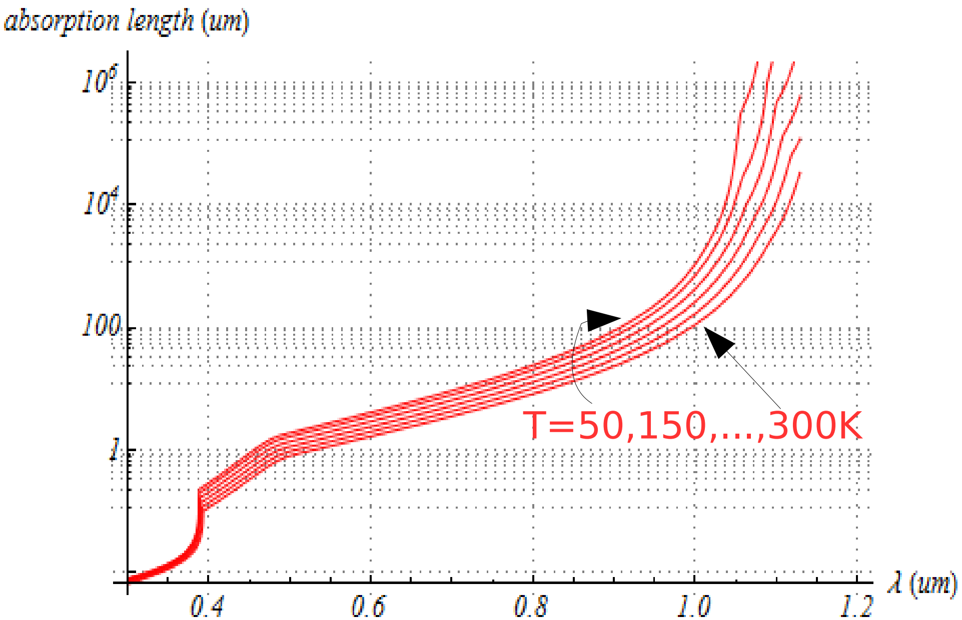

Rajkanan et al, Solid State Ele 22 (1979) 793

Accounting E_{gap} variations with T, etc...

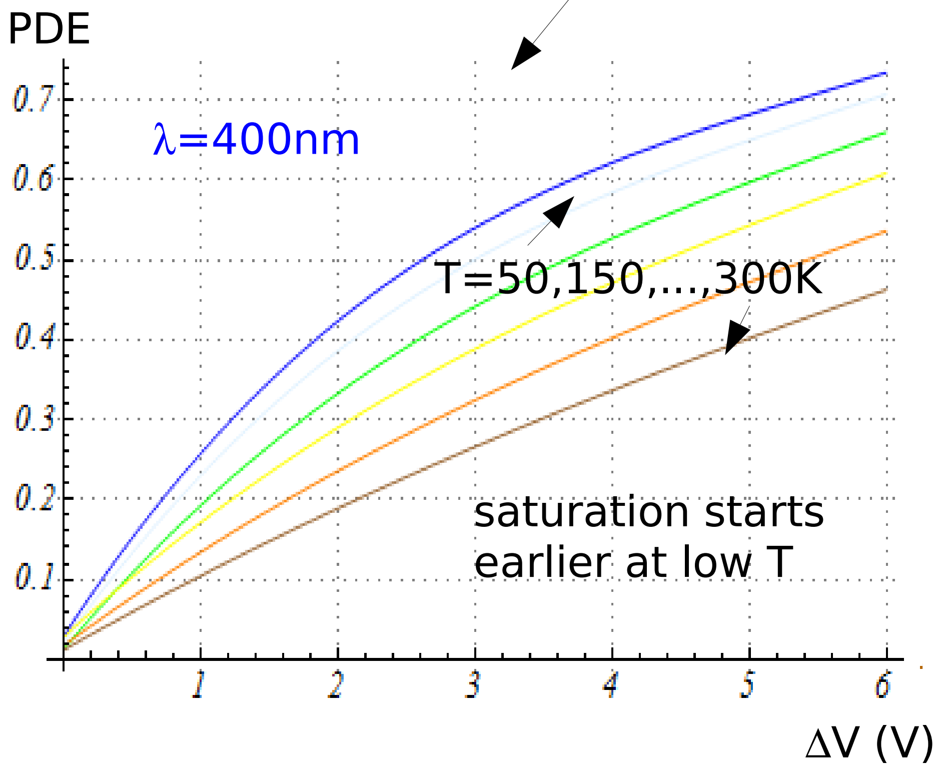

Understanding PDE vs T: 1D model

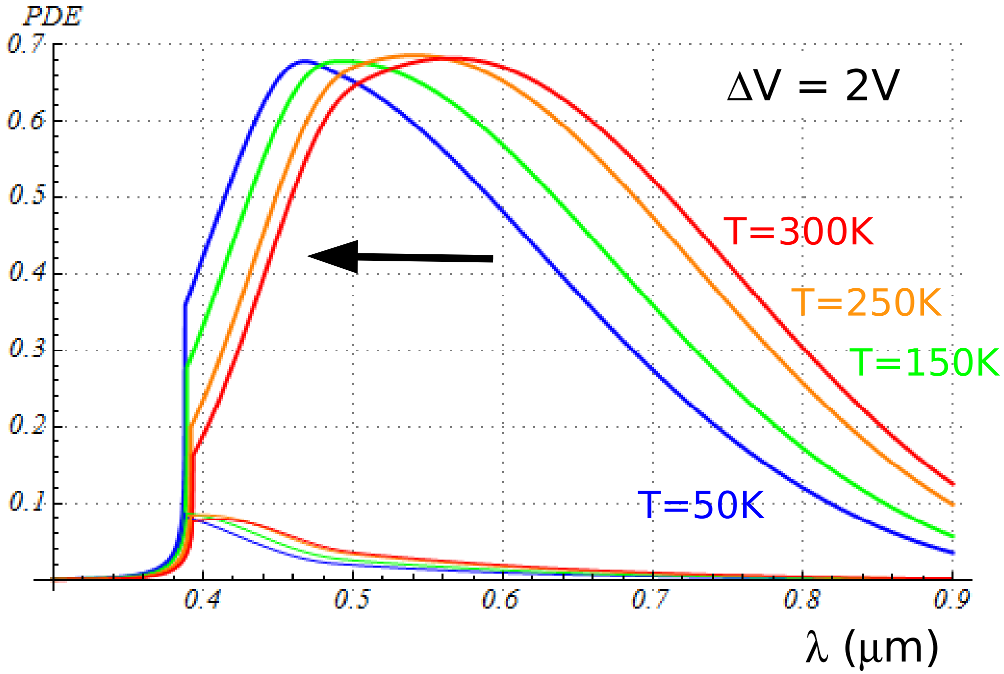

1) main contribution to PDE from electrons → PDE distribution shifted toward short λ at low T because of larger absorption length (photo-generation deeper into depletion layer → gain for shorter λ, loss for longer λ)

(see also PDE vs T)

2) tunneling effects not included in the model (enhancement of PDE, interplay with band gap variations with T)

3) freeze-out not included in the model

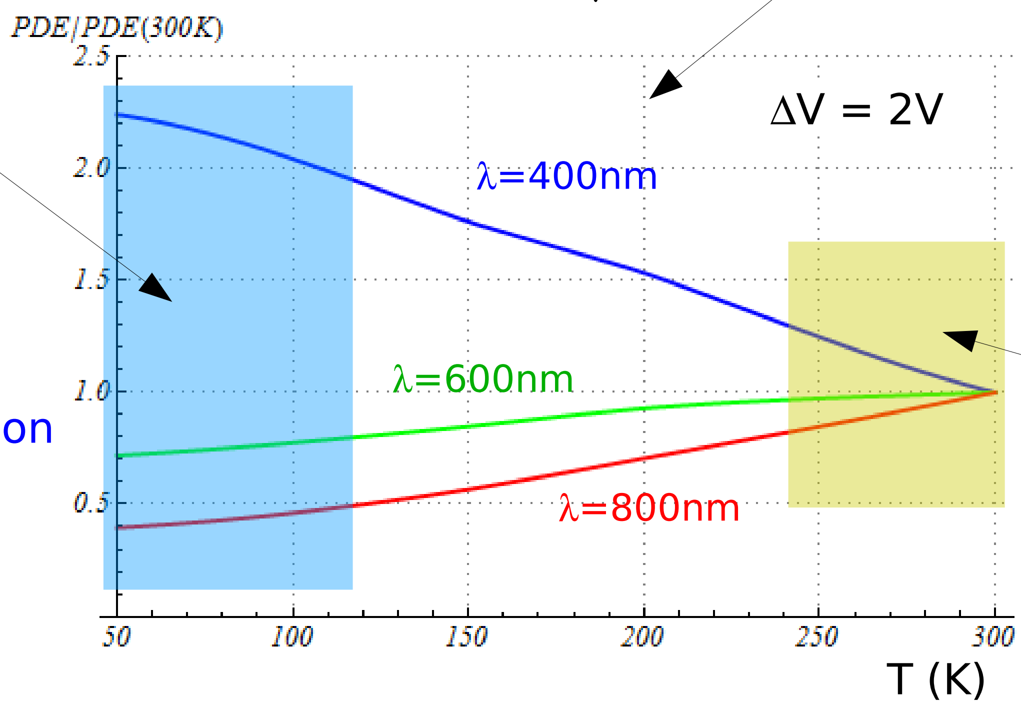

4) something else is missing: need to explain PDE decreasing with T for 250K<t<300K

5) Recombination not includedl

to be understood !

Overview – SiPM timing properties

- Intrinsic timing: discussion of intrinsic timing properties based on measurements of single photon timing resolution

G.C. et al NIMA 581 (2007) 461
and paper in preparation

- A few comments about timing related to signal shape

GM-APD avalanche development

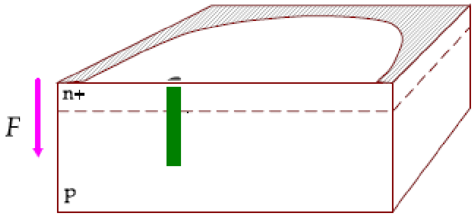

Longitudinal multiplication

- Duration ~ few **ps**
- Internal current up to ~ few **µA**

(1) Avalanche "seed": free-carrier concentration rises exponentially by **"longitudinal" multiplication**

(1') Electric field locally lowered (by **space charge effect**) towards breakdown level

Multiplication is self-sustaining
Avalanche current steady until new multiplication triggered in near regions

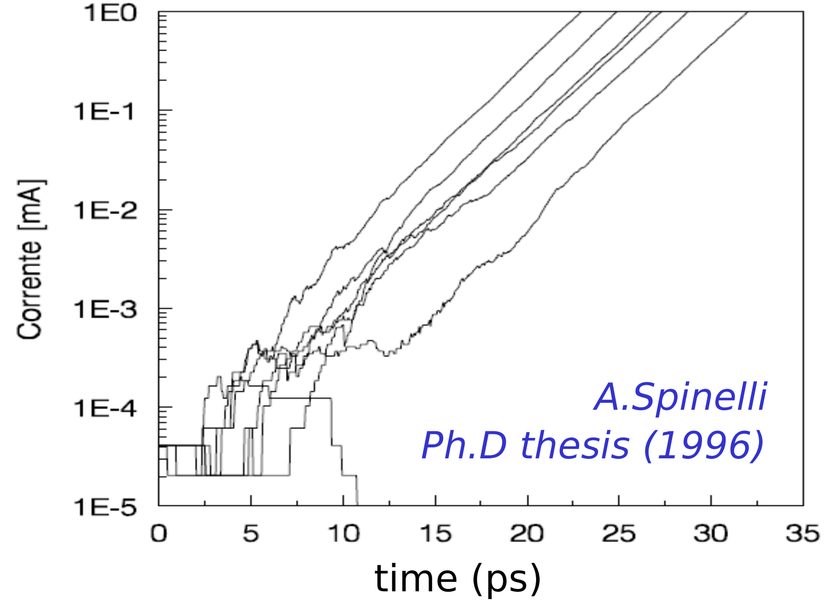

x100

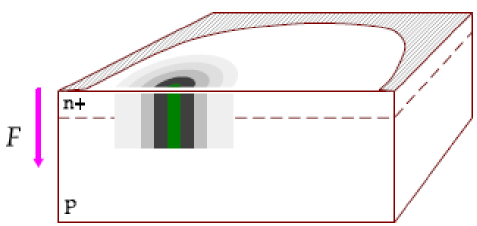

Transverse multiplication

- Duration ~ few **100ps**
- Internal current up to ~ several **10µA**

(2) Avalanche spreads "transversally" across the junction

(**diffusion speed ~up to 50µm/ns** enhanced by multiplication)

(2') Passive quenching mechanism effective after transverse **avalanche size ~10µm**

(Otherwise avalanche spreads over the whole active depletion volume
→ avalanche current reaches a final saturation steady state value)

Simulation w/o quenching:
→ steady current reached

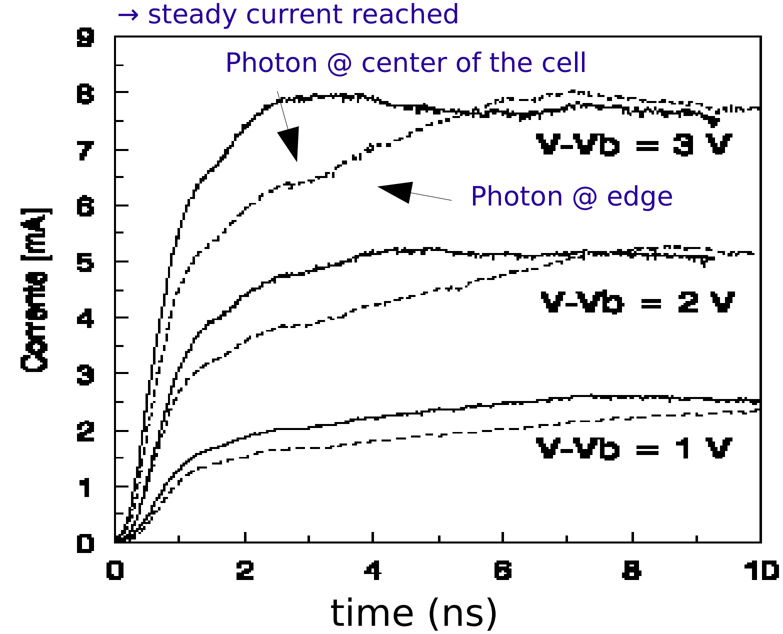

GM-APD avalanche transverse propagation

Avalanche transverse propagation by a kind of shock wave: the wavefront carries a high density of carriers and high E field gradients (inside: carriers' density lower and E field decreasing toward breakdown level)

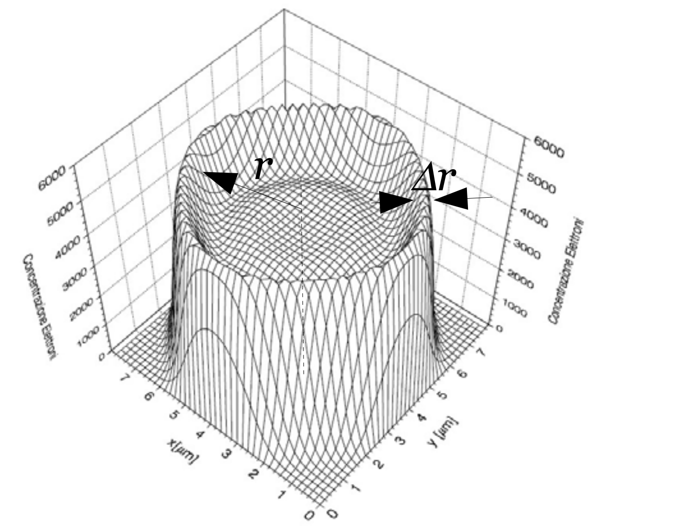

$$\frac{dS}{dt} = \frac{d}{dt} 2\pi r(t)\Delta r = 2\pi v_{diff}\Delta r = 4\pi\Delta r\sqrt{\frac{D}{\tau}}$$

Rate of current production: $$\frac{dI}{dt} = \frac{dI}{dS}\frac{dS}{dt} \sim \frac{\sqrt{D}}{R_{sp}\sqrt{\tau}}$$

$$\frac{dI}{dS} = J = \frac{V_{bias}}{R_{sp}(S)}$$

S = surface of wavefront (ring of area $2\pi r\Delta r$)

$R_{sp}(S)$ = space charge resistance $\sim w^2/2\varepsilon v \sim O(50\ k\Omega\ \mu m^2)$

$v_{diff} \sim$ O(some 10μm/ns)

D = transverse diffusion coefficient ~ O(μm^2/ns)

τ = longitudinal (exponential) buildup time ~ O(few ps)

(Internal) current rising front:
the faster it grows, the lower the jitter
dI/dt → understand/engineer timing features of SiPM cells

$$\tau \sim \frac{1}{1-(E_{max}/E_{breakdown})^n}$$

→ timing resolution improves at high V_{bias}

→ E field profile affects τ and R_{sp} (wider E field profile → smaller R) (should be engineered when aiming at ultra-fast timing)

→ T dependence of timing through τ and D

→ slower growth at GAPD cell edges → higher jitter at edges reduced length of the propagation front

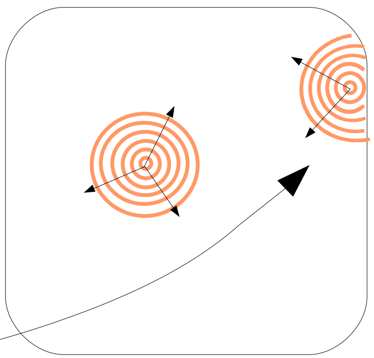

SiPM cell

GM-APD timing jitter: fast and slow components

1) Fast component: gaussian with time scale O(100ps)

Statistical fluctuations in the avalanche:

- **Longitudinal** build-up (minor contribution)
- **Transversal** propagation (main contribution):

  - via multiplication assisted diffusion (dominating in few μm thin devices) *A.Lacaita et al. APL and El.Lett. 1990*

  - via photon assisted propagation (dominating in thick devices – O(100μm)) *PP.Webb, R.J. McIntyre RCA Eng. 1982* *A.Lacaita et al. APL 1992*

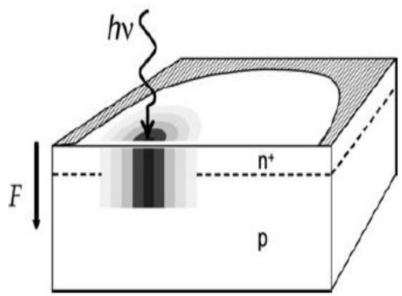

Multiplication assisted diffusion

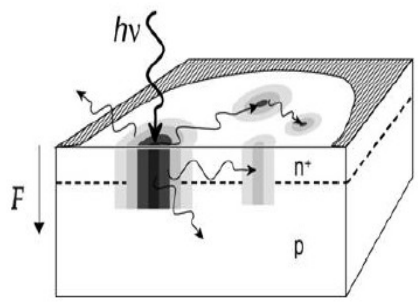

Photon assisted propagation

Fluctuations due to
a) impact ionization statistics

→ Jitter at minimum → O(10ps)
(very low threshold → not easy)

b) depth of photo-generation position due to finite drift time in low E field region (even at saturated velocity)

→ note: saturated $v_e \sim 3\ v_h$

Fluctuations due to
a) variance of the transverse diffusion speed v_{diff}

b) injection position statistics

→ Jitter → O(100ps)
(usually threshold set high)

GM-APD timing jitter: fast and slow components

2) Slow component: non-gaussian tails with time scale O(ns)

Carriers photo-generated in the neutral regions above/beneath the junction and reaching the electric field region by diffusion

G.Ripamonti, S.Cova Sol.State Electronics (1985)

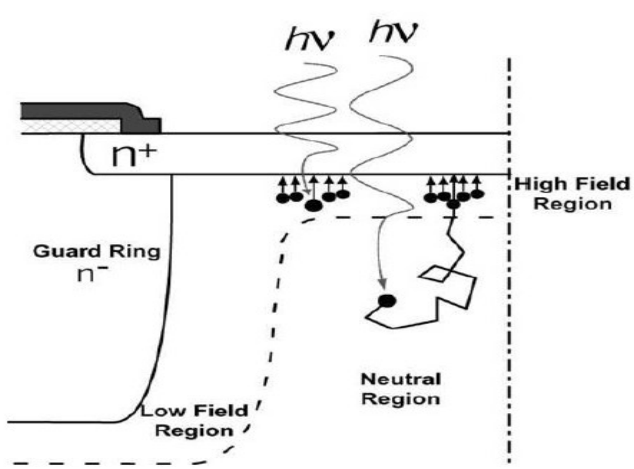

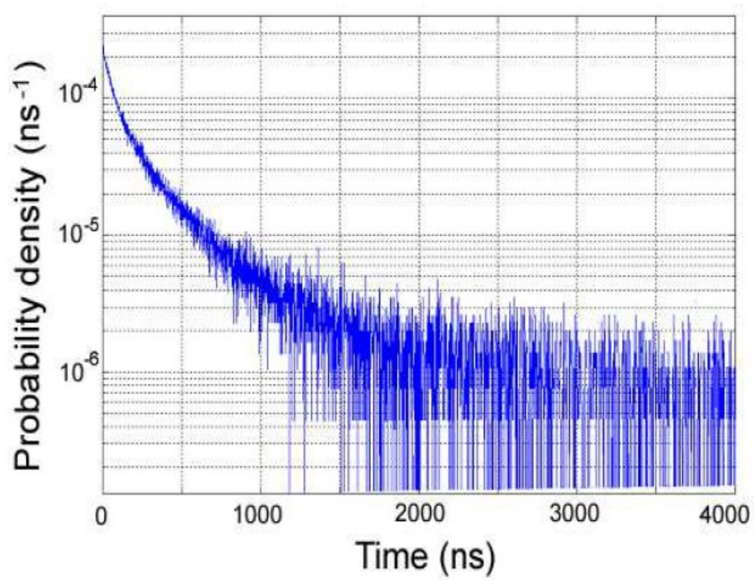

tail lifetime: $\tau \sim L^2 / \pi^2 D$ ~ up to some ns
L = effective neutral layer thickness
D = diffusion coefficient

S.Cova et al. NIST Workshop on SPD (2003)

Neutral regions underneath the junction : timing tails for long wavelengths

(Neutral regions in APD entrance: timing tails for short wavelengths)

Measurements - experimental setup

Pump Laser
Millenia V (Spectra-physics)
solid state CW visible laser

Crystal for Second Harmonic Generation (SHG)
conversion 800 nm → 400 nm
efficiency at % level

Low noise LV suppliers

LeCroy SDA 6020
Analog bandwidth: 6GHz
Sampling rate: 20GS/s
Vertical resolution: 8 bits

External trigger from Ti:sappire laser signal

Mode-locked Ti:sapphire Laser
Tsunami (Spectra-physics)
femtosecond pulsed laser

Filters
blue + neutral
for rejecting IR light and tune intensity

wavelength: tuned at 800±15 nm
pulse width: ~ 60 fs FWHM
pulse period: ~ 12 ns
pulse timing jitter < 100 fs

Electronics
I → V conversion via R_L (500Ω)
Two stage voltage amplification (= x50) based on high-bandwidth low-noise RF amplifier: gali-5 (MiniCircuits)
Z_{in}= 50Ω

Data taking conditions:

- different V_{bias}
- both at 800 nm and 400 nm
- with different light intensities (counting rates in the range 10÷20 Mhz ie 15÷30 KHz per single cell)

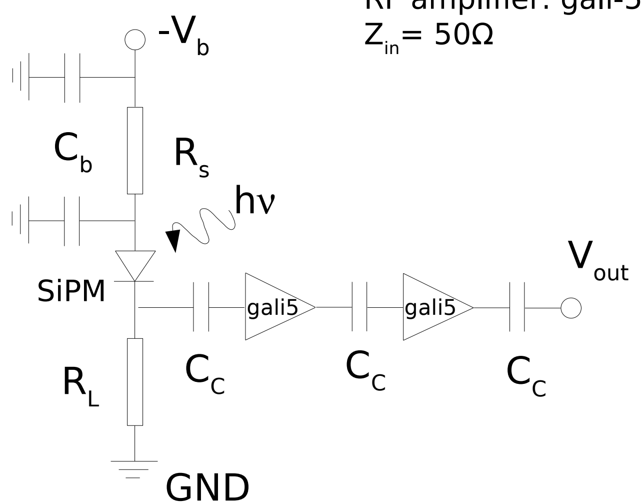

Waveform analysis: method

(1) Selection of candidate peaks:
- single photon peaks
- proper signal shape
- low instantaneous intensity (no activity before/after within 50ns)
- low noise during the previous 10 ns (typical noise ~ 1mV rms)

(2) Peak reconstruction
- optimum time reconstruction
- amplitude and width (baseline shift correction)

(3) Time difference Δt between consecutive peaks

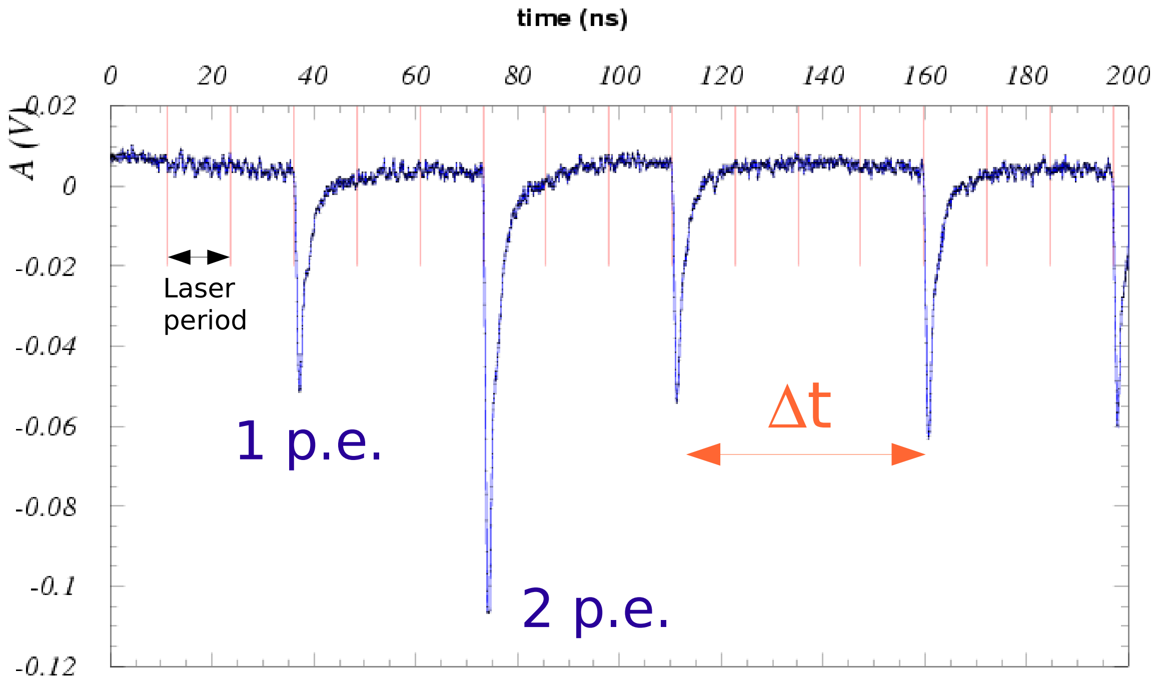

NOTE: good timing properties even up to 10MHz/mm^2 photon rates

Waveform (1 p.e.)

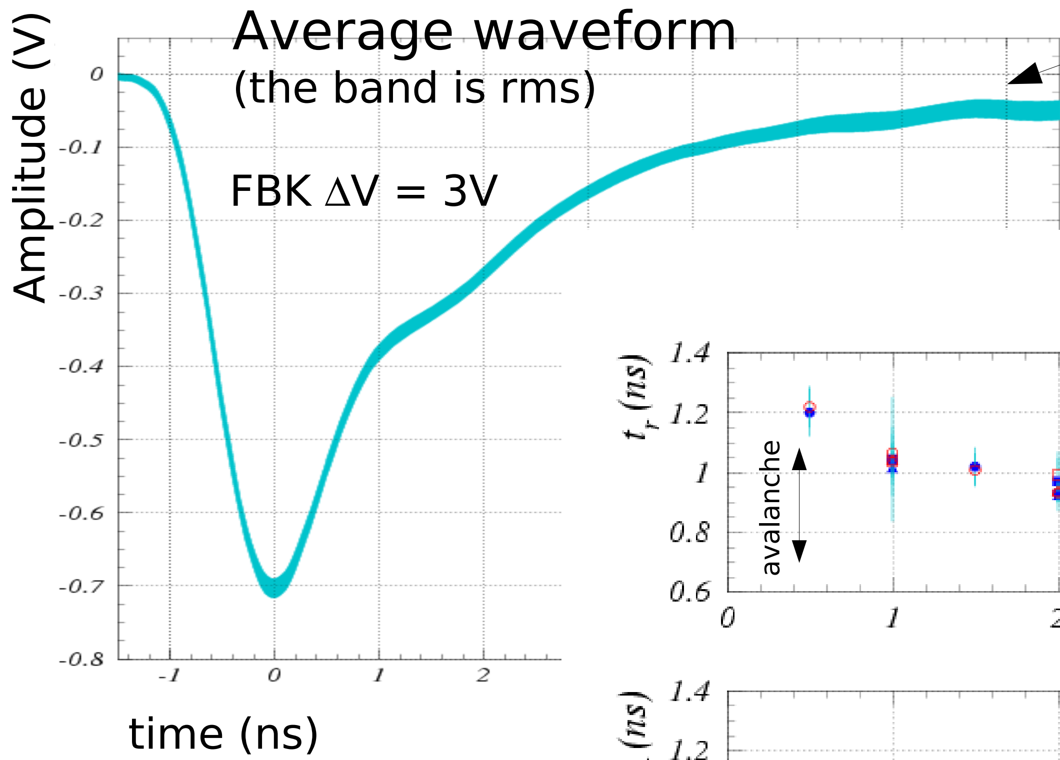

Additional contribution to rms (afterpulses)

Risetime (10%-90%)

(dominated by electronics contribution)

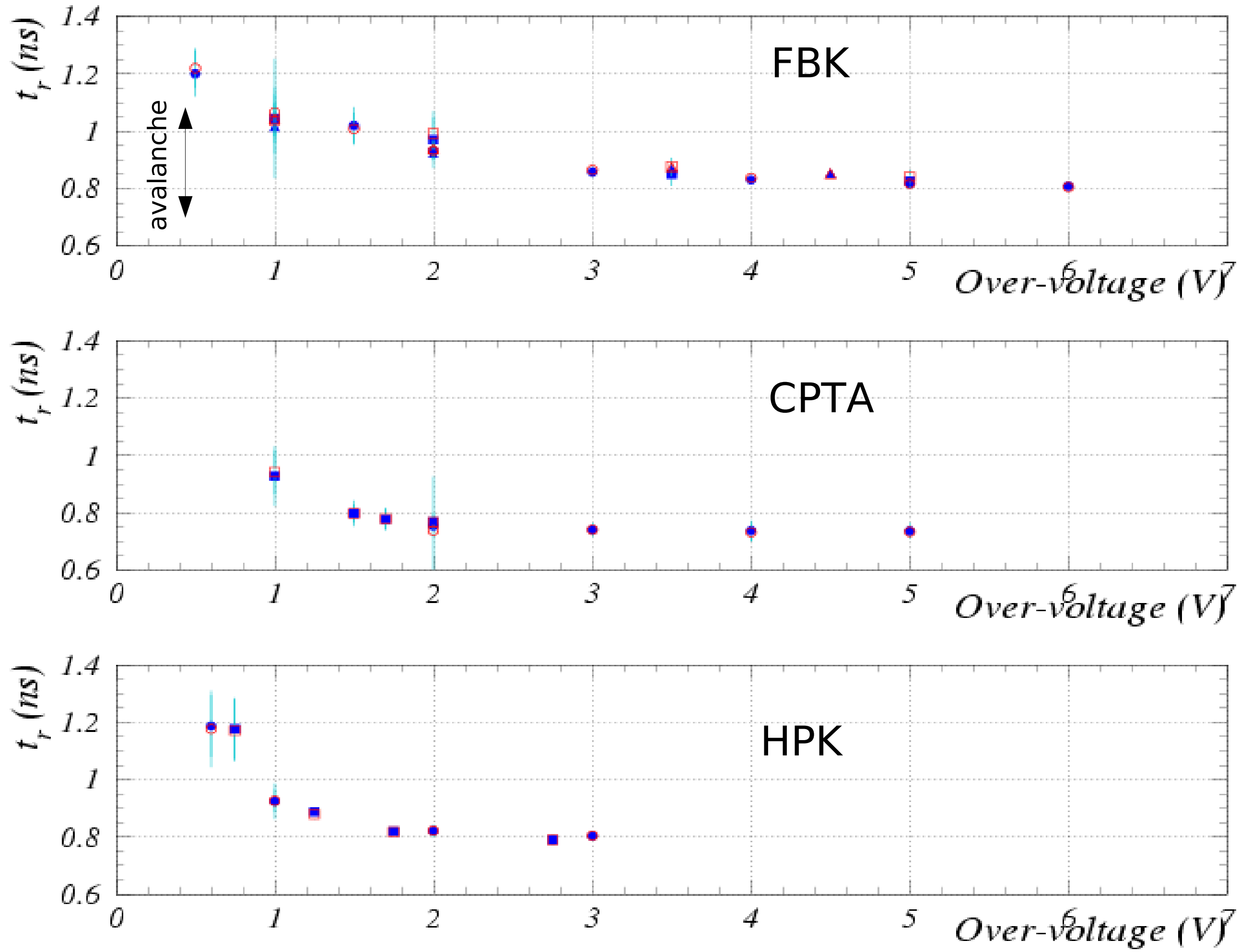

Note:

$$\frac{dI}{dt} \sim \frac{\sqrt{D}}{R_{sp}\sqrt{\tau}}$$

$$\tau \sim \frac{1}{1-(E_{max}/E_{breakdown})^n}$$

Waveform analysis: optimum timing filter

Different methods to reconstruct the time of a peak:

✗ parabolic fit to find the peak maximum
✗ average of time samples weighted by the waveform derivative
✔ digital filter: weighting by the derivative of a reference signal
→ optimum against (white) noise (if signal shape fixed)

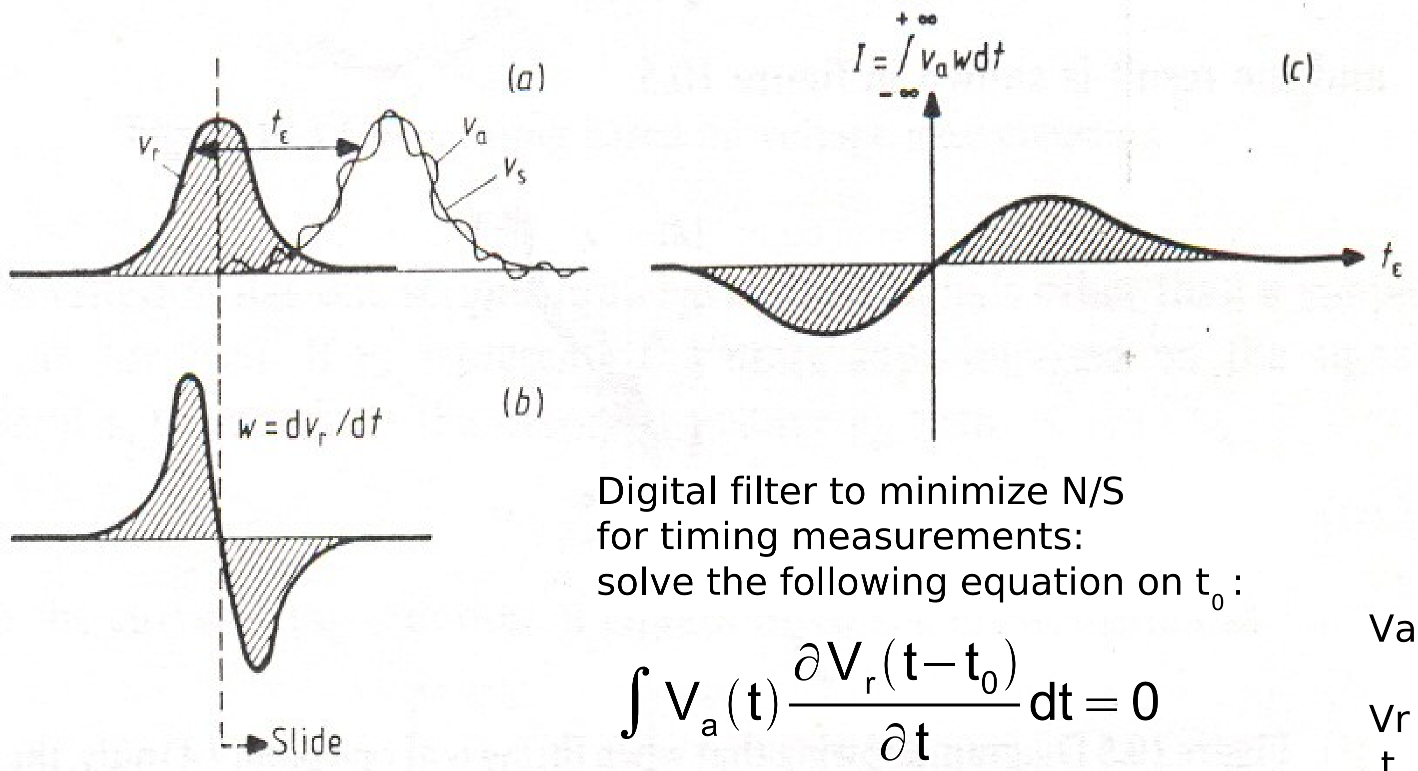

Digital filter to minimize N/S
for timing measurements:
solve the following equation on t_0:

$$\int V_a(t) \frac{\partial V_r(t-t_0)}{\partial t} dt = 0$$

Va = measured signal
(includes noise)
Vr = reference signal
t_0 = reference time

see e.g. Wilmshurst "Signal recovery from noise in electronic instrumentation"

Single Photon Timing Resolution (SPTR)

Analysis of the distributions of the t difference between successive peaks (modulo the laser period T_{laser}=12.367ns)

Gaussian + Tails (long λ)

rms~50-100 ps

~ exp (-t / O(ns))
contrib. several %
for long wavelengths

Data at λ=400nm
fit gives reasonable χ^2
with gaussian (σ_t^{fit}) +
constant term (dark noise contribution)

The detector resolution is obtained by
$\sigma_t^{fit}/\sqrt{2}$

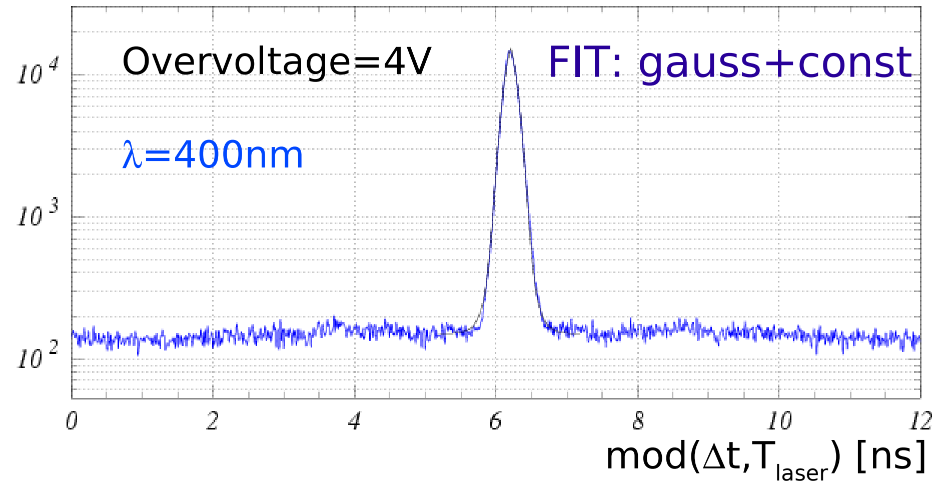

Data at λ=800nm
fit gives reasonable χ^2 in case of an additional exponential term $\exp(-|\Delta t|/\tau)$

- $\tau \sim$ 0.2÷0.8ns in rough agreement with diffusion tail lifetime: $\tau \sim L^2 / \pi^2 D$ if L is taken to be the diffusion length
- Contribution from the tails ~ 10÷30% of the resolution function area

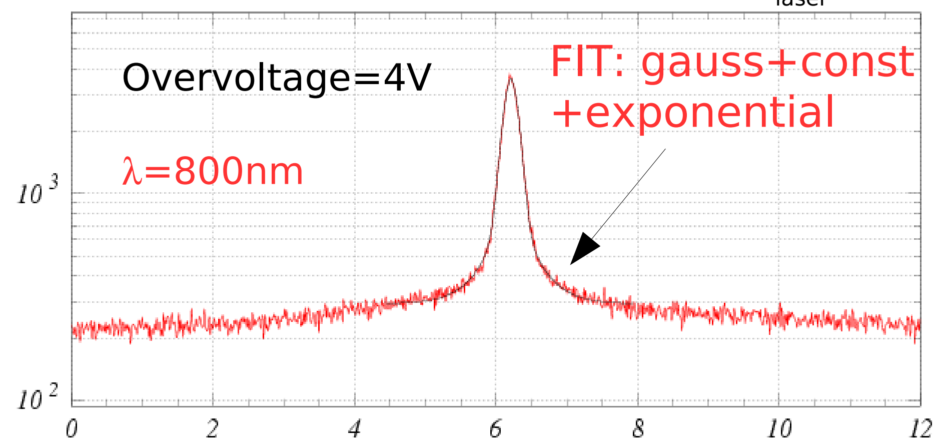

Distributions of the difference in time between successive peaks (modulo the measured laser period T_{laser}=12.367ns)

FBK – single photon timing res. (SPTR)

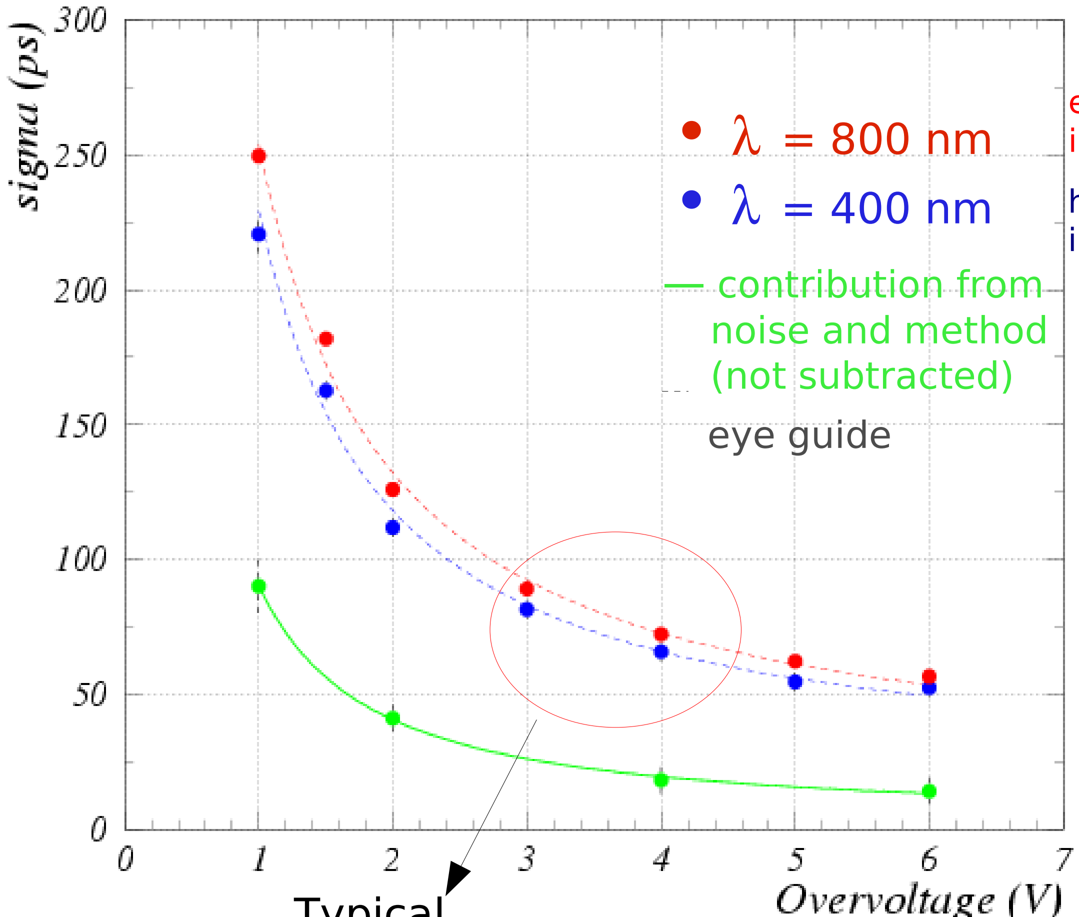

Better resolution for short wavelengths: carriers generated next to the high E field region

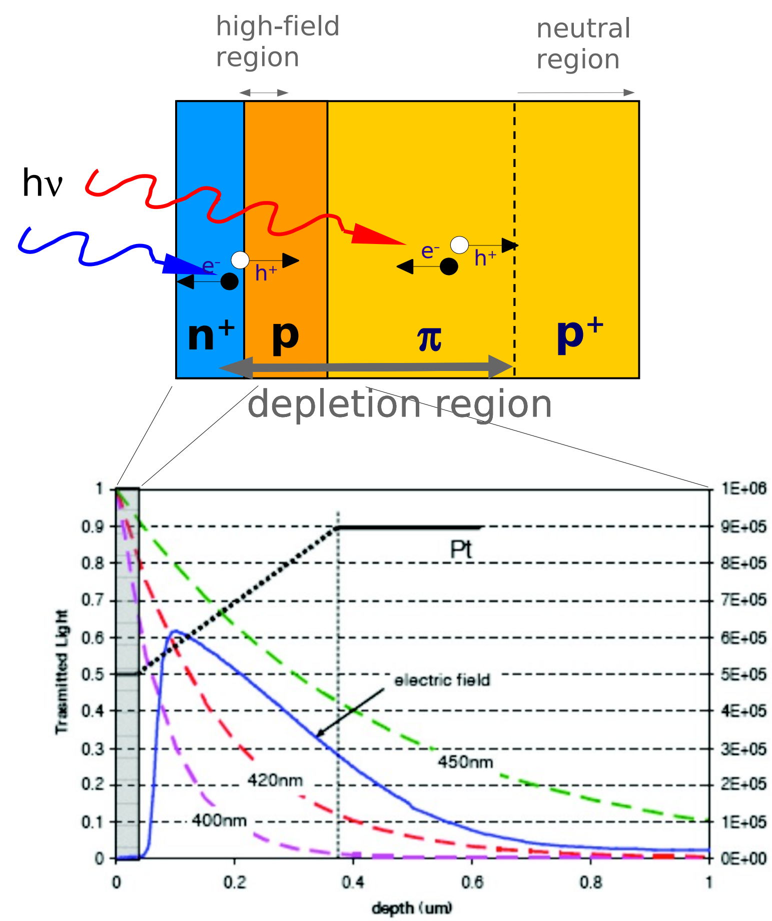

G.Collazuol et al NIMA 581 (2007) 461

FBK devices - shallow junction

SiPM type without optical trench | SiPM type with optical trench

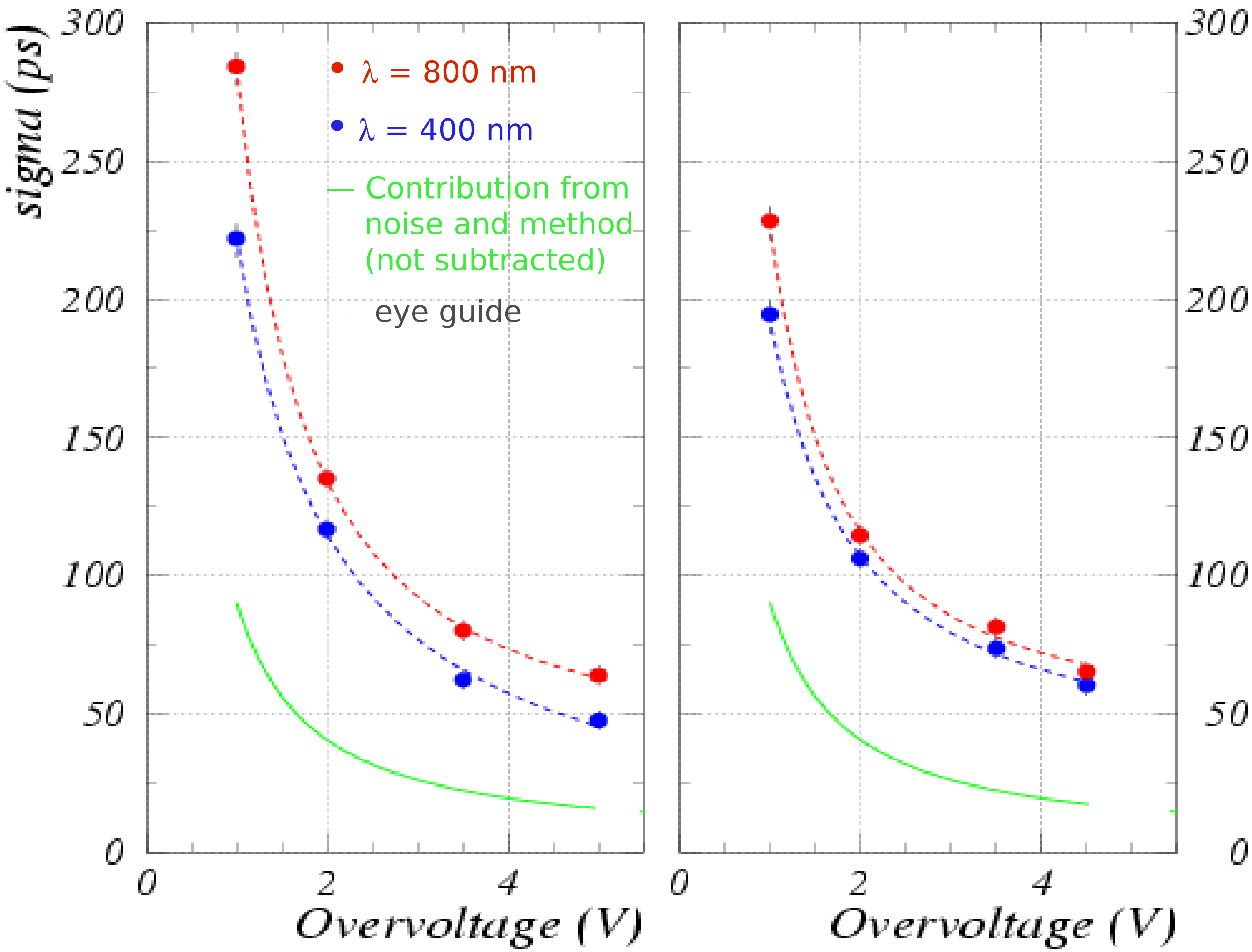

FBK

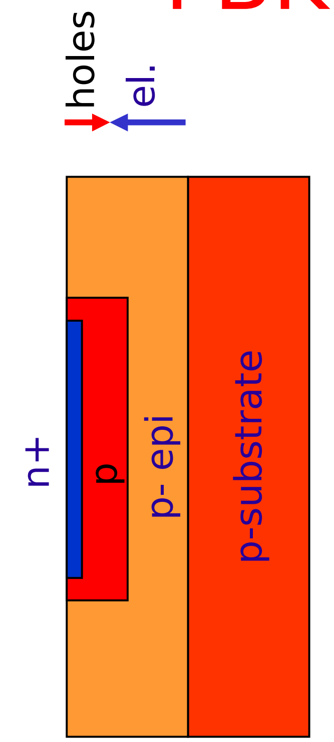

(Devices with the same high field structure)

Hamamatsu - shallow junction

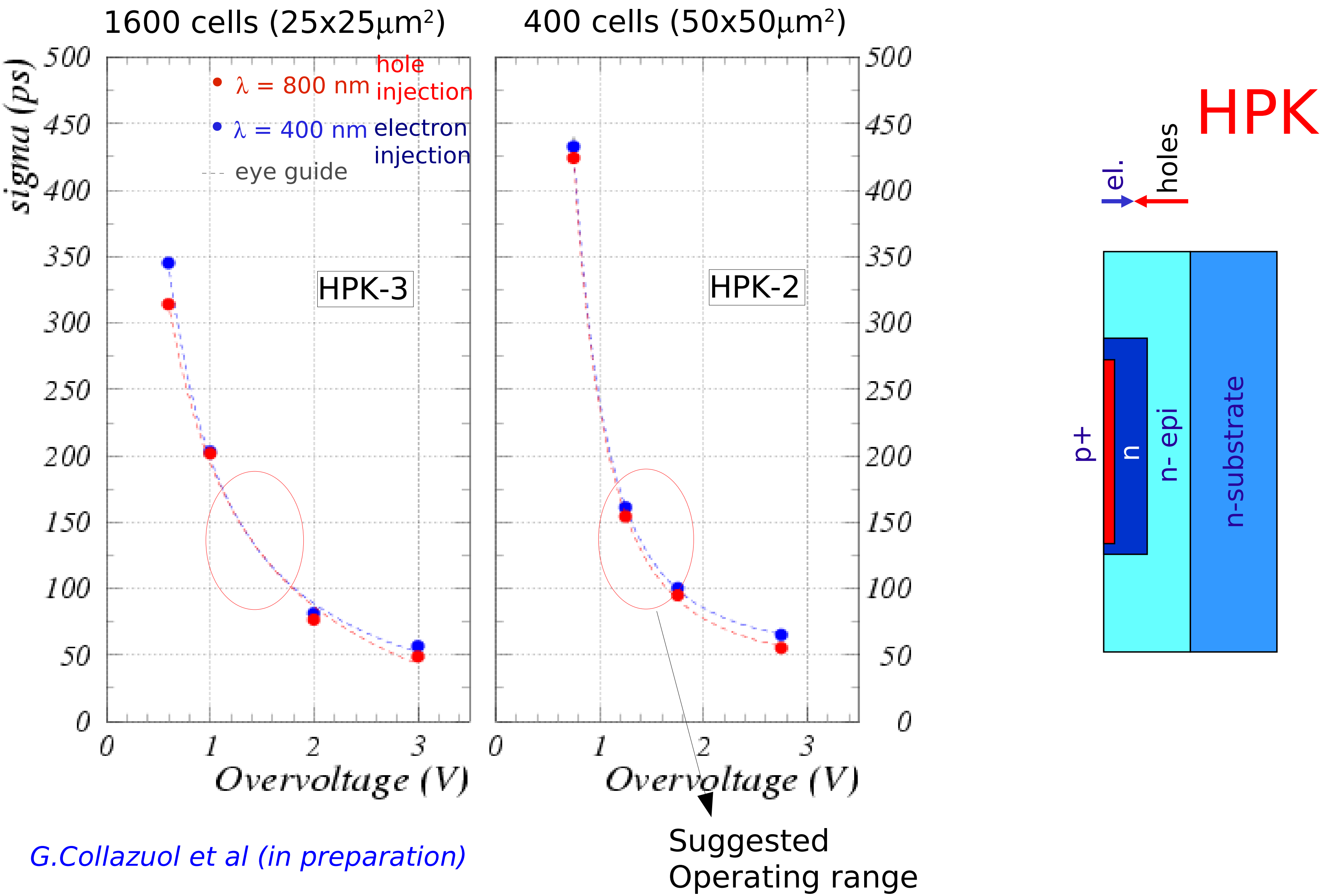

G.Collazuol et al (in preparation)

CPTA/Photonique - deep junctions

a) Green-Red sensitive
SSPM 050701GR_TO18

b) Blue sensitive
SSPM 050901B_TO18

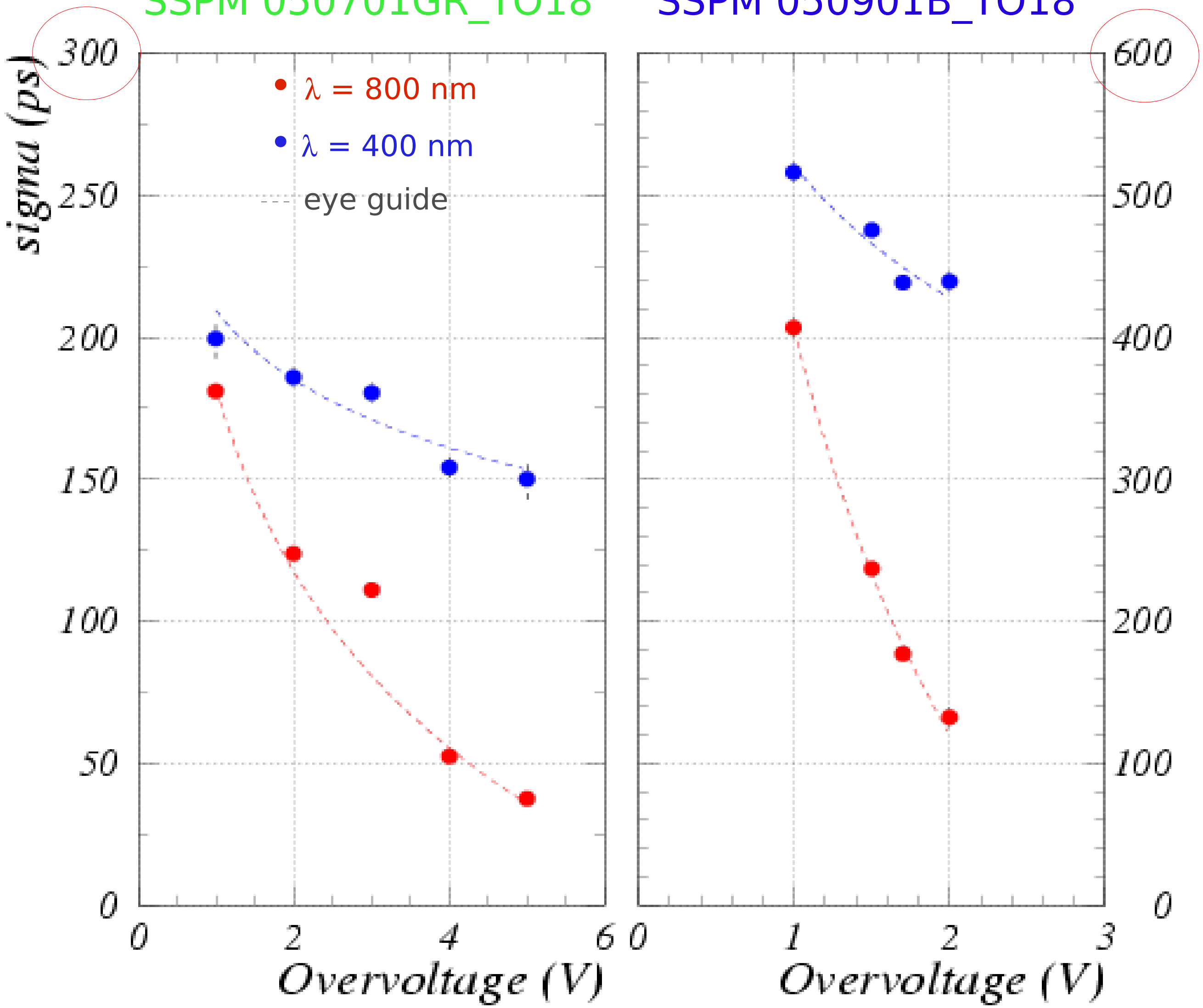

Thick structures,
buried junctions ?

a) n^+/p
→ electrons drift

b) p^+/n
→ holes drift ($v_e/3$)

SPTR: position dependence

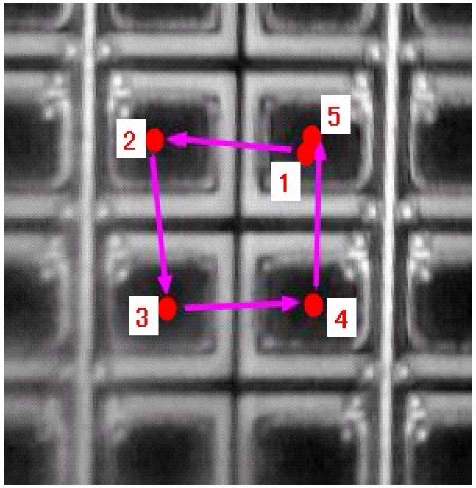

	FWHM (ps)	FWTM (ps)
1	199	393
2	197	389
3	209	409
4	201	393
5	195	383

K.Yamamoto PD07

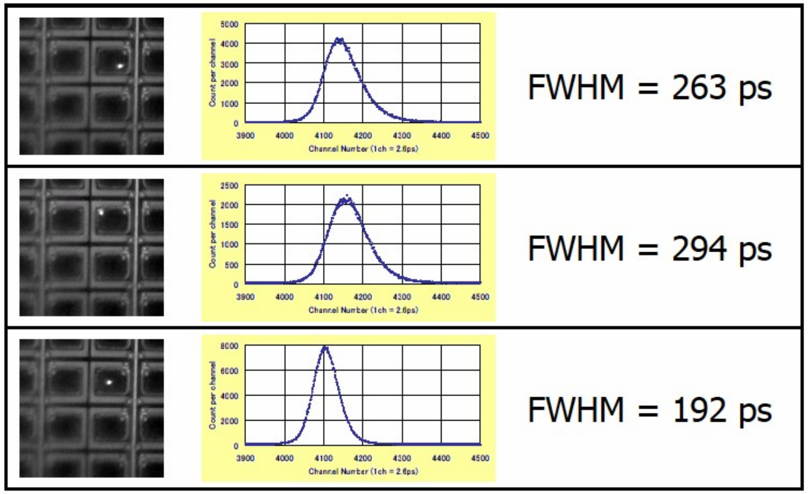

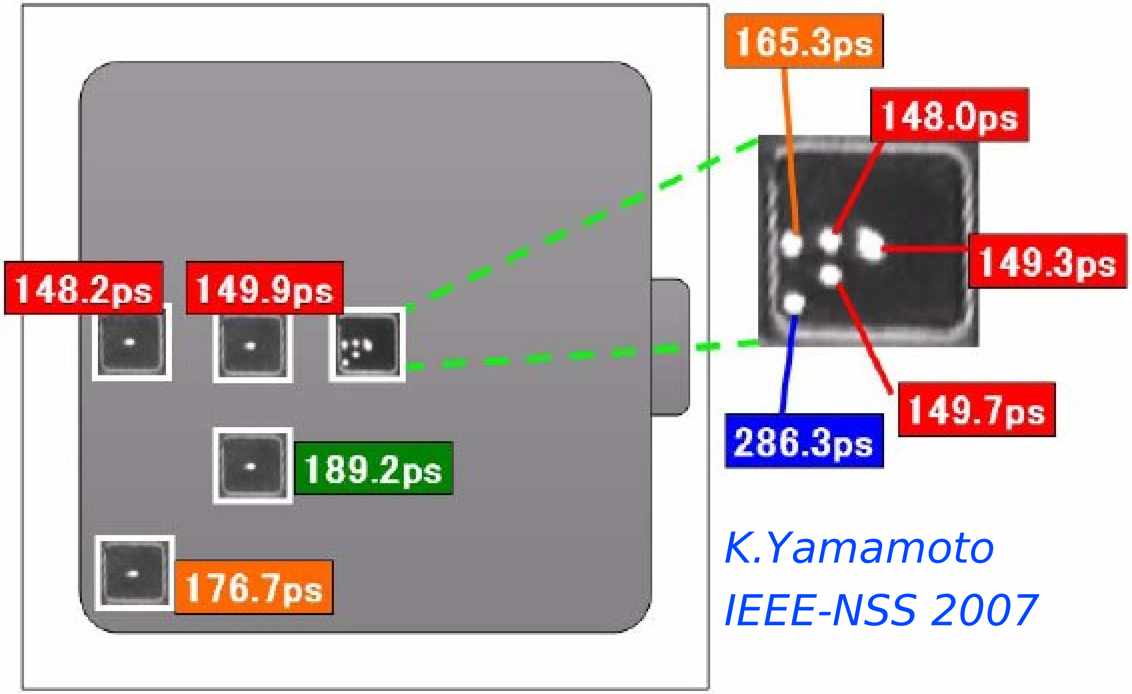

K.Yamamoto IEEE-NSS 2007

Larger jitter if photo-conversion at the border of the cell

Due to:
1) slower avalanche front propagation

2) lower E field at edges

→ cfr PDE vs position

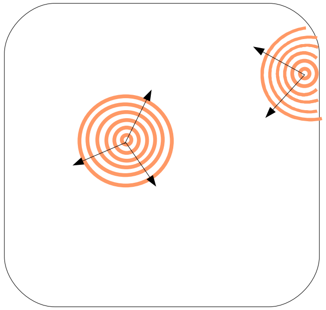

Data include the system jitter (common offset, not subtracted)

SPTR: timing at low T

Timing: improves at low T

Lower jitter at low T due to higher mobility: → a) avalanche process is faster; b) reduced fluctuations

(Over-voltage fixed)

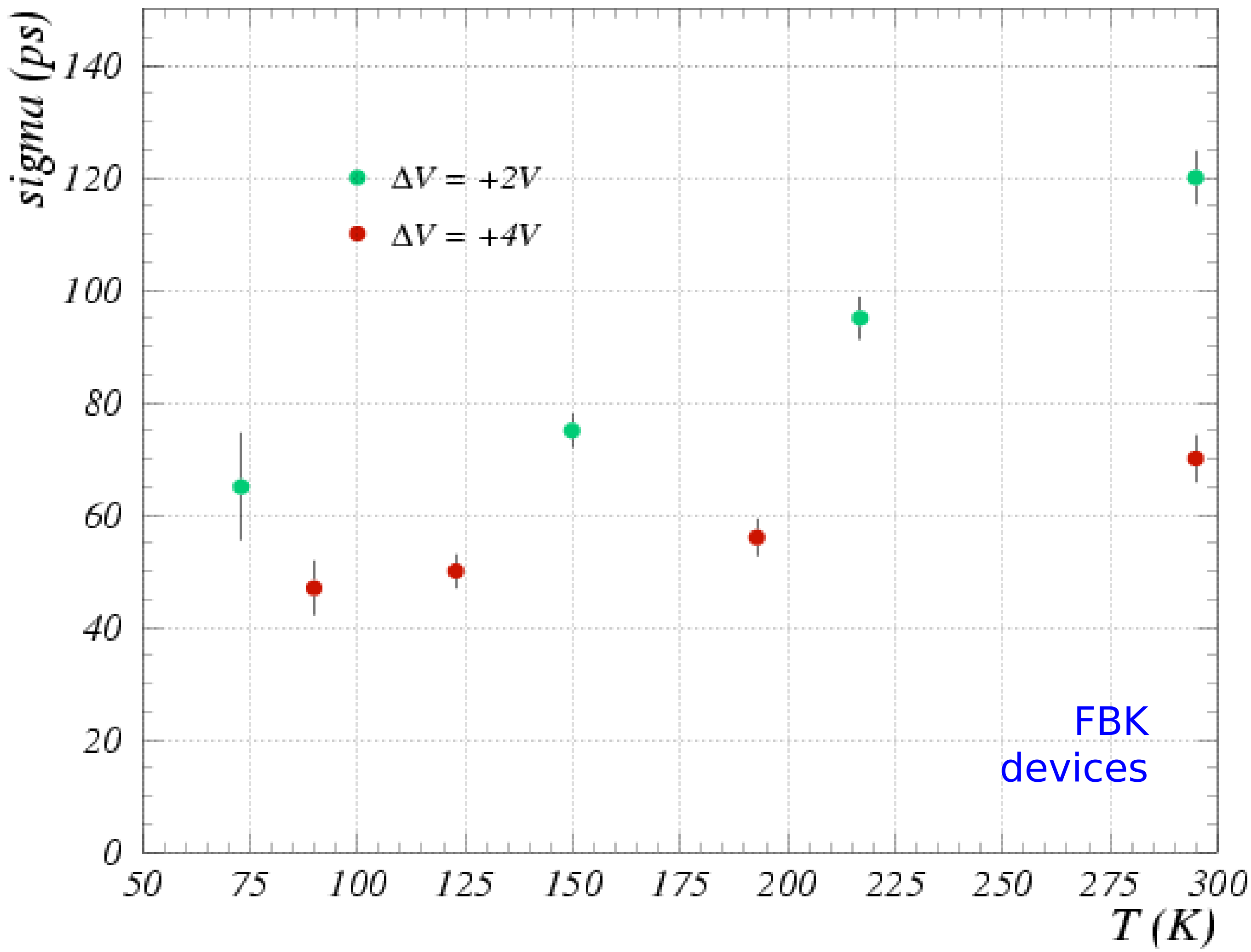

G.C. (2011, unpublished)

Setup:
- Cryo-cooler setup described before
- PicoQuant laser (40ps FWHM, λ~405nm)
- Wide band amplifier (used for timing measurements)

Note:

$$\frac{dI}{dt} \sim \frac{\sqrt{D}}{R_{sp}\sqrt{\tau}}$$

Timing properties → fast timing devices

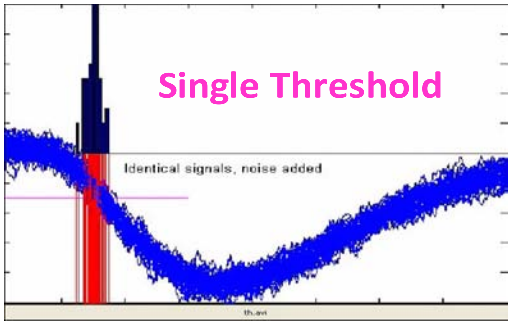

Timing by (single) threshold:

→ time spread proportional to 1/rise-time and noise

$$\sigma_{time} = \frac{\sigma_{amplitude}}{\frac{df(t)}{dt}}$$

Timing with optimum filtering:

→ best resolution with f'(t) weighting function

$$\sigma^2_{time} = \frac{\sigma^2_{amplitude}}{\int dt \left[\frac{df(t)}{dt}\right]^2}$$

Pulse sampling and Waveform analysis:

Sample, digitize, fit the (known) waveform
→ get time and amplitude

$$\sigma^2_{time} = \frac{\sigma^2_{amplitude}}{N_{samples} \int dt \left[\frac{df(t)}{dt}\right]^2}$$

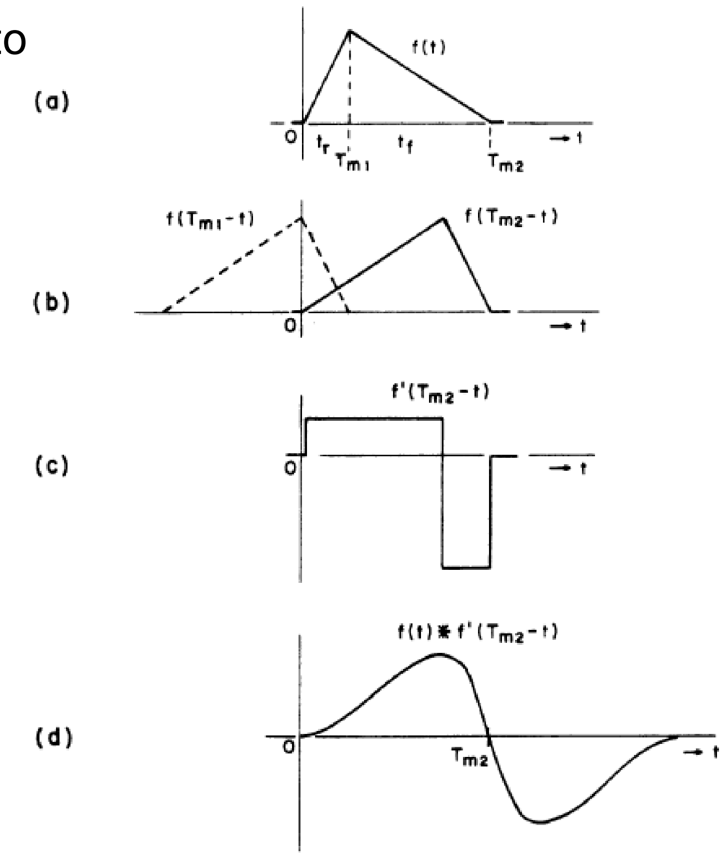

Fig. 7. Optimum filter for timing in presence of white noise (method of derivation).
(a) signal waveform
(b) optimum filter for amplitude measurements.
(c) optimum filter for timing - derivative of (b).
(d) output waveform.

V.Radeka IEEE TNS 21 (1974) and vast literature thereafter

SiPM equivalent circuit

Single cell model → $(R_d||C_d)+(R_q||C_q)$

SiPM + load → $(||Z_{cell})||C_{grid} + Z_{load}$

Signal = slow pulse ($\tau_{d\ (rise)}, \tau_{q\text{-}slow\ (fall)}$) +

+ fast pulse ($\tau_{d\ (rise)}, \tau_{q\text{-}fast\ (fall)}$)

- $\tau_{d\ (rise)} \sim R_d(C_q+C_d)$
- $\tau_{q\text{-}fast\ (fall)} = R_{load}\ C_{tot}$ (fast; parasitic spike)
- $\tau_{q\text{-}slow\ (fall)} = R_q\ (C_q+C_d)$ (slow; cell recovery)

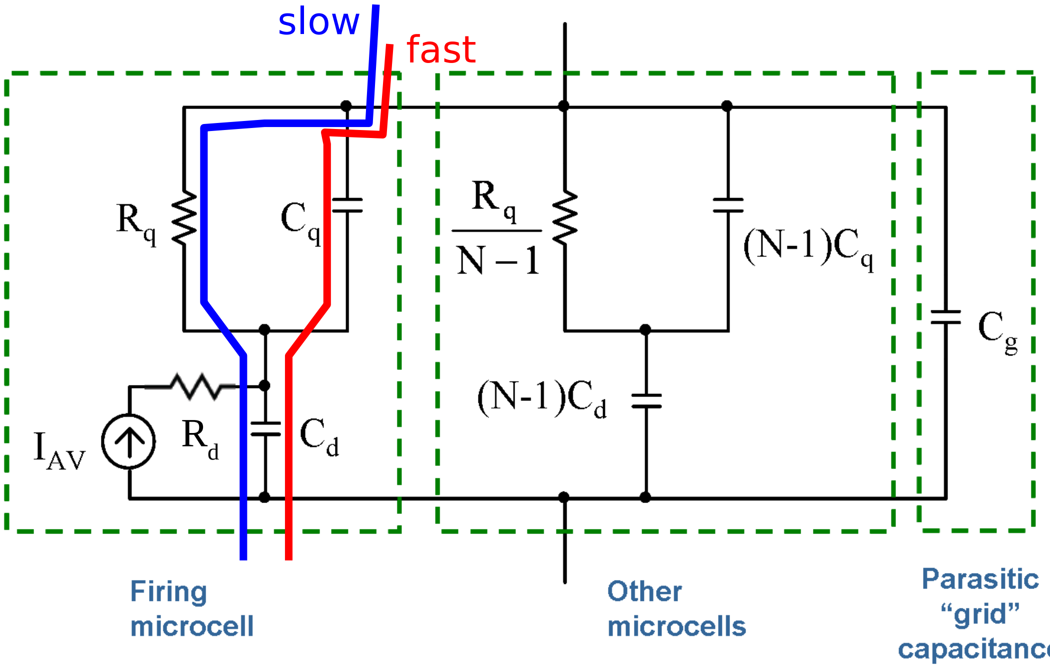

Pulse shape

$$V(t) \simeq \frac{Q}{C_q+C_d}\left(\frac{C_q}{C_{tot}} e^{\frac{-t}{\tau_{FAST}}} + \frac{R_{load}}{R_q}\frac{C_d}{C_q+C_d} e^{\frac{-t}{\tau_{SLOW}}}\right)$$

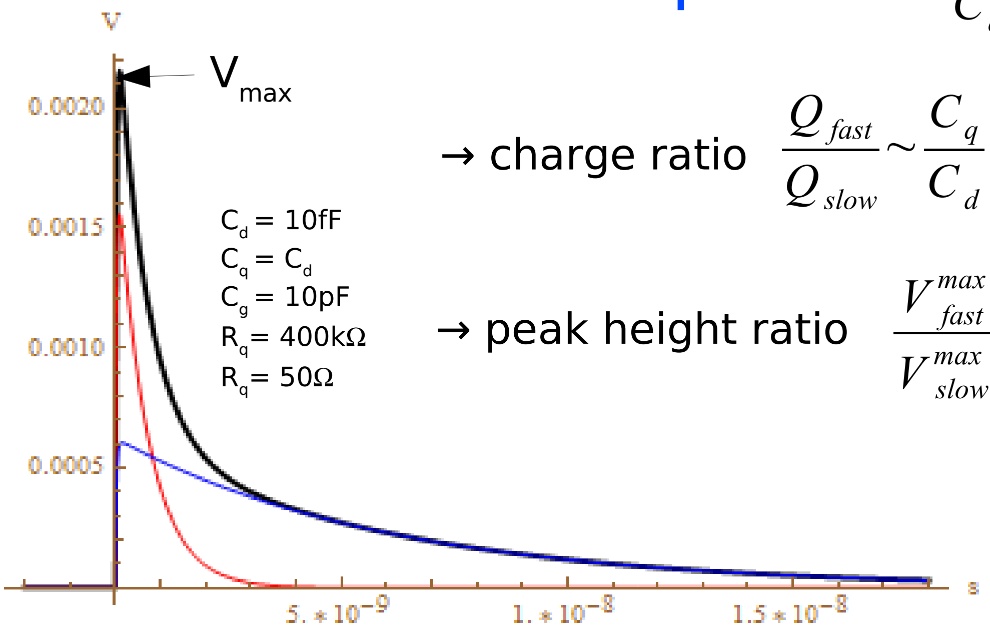

→ charge ratio $\frac{Q_{fast}}{Q_{slow}} \sim \frac{C_q}{C_d}$

→ peak height ratio $\frac{V_{fast}^{max}}{V_{slow}^{max}} \sim \frac{C_q^2 R_q}{C_d C_{tot} R_{load}}$

increasing with Rq and $1/R_{load}$ (and Cq of course)

Optimizing signal shape for timing (SPTR)

→ peak height ratio $\frac{V_{fast}^{max}}{V_{slow}^{max}} \sim \frac{C_q^2 R_q}{C_d C_{tot} R_{load}}$

Enhancing C_q does improve timing performances

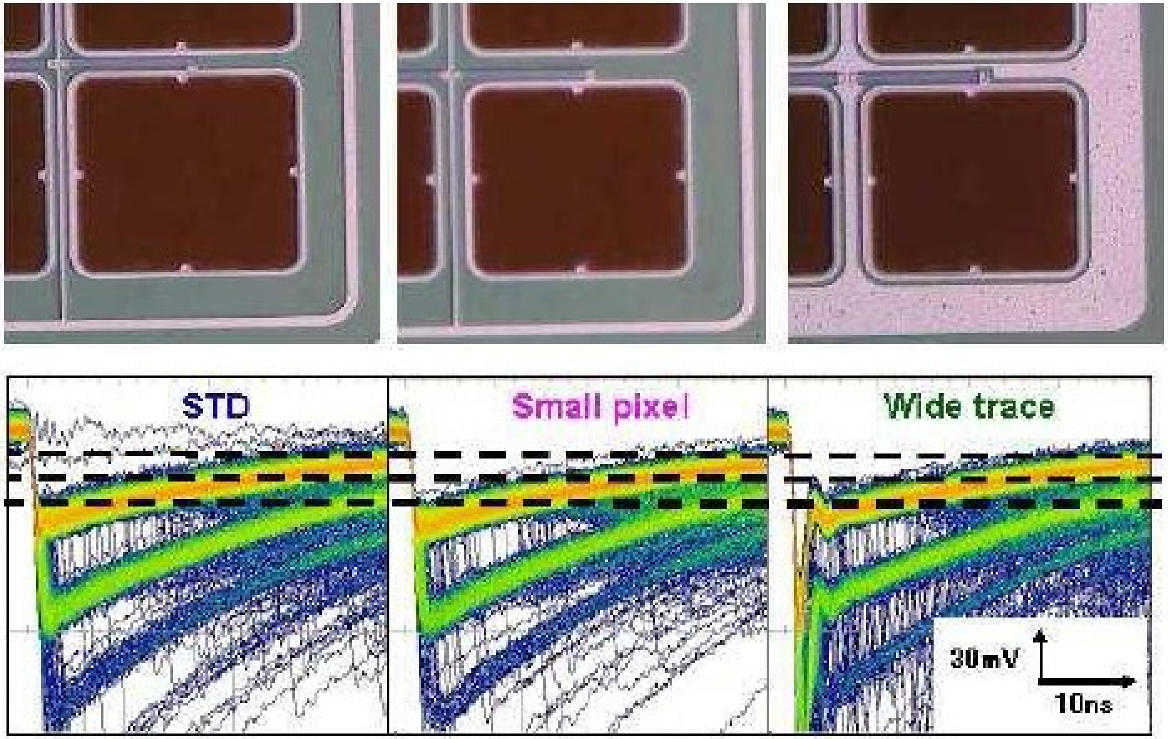

Yamamura et.al. at PD09

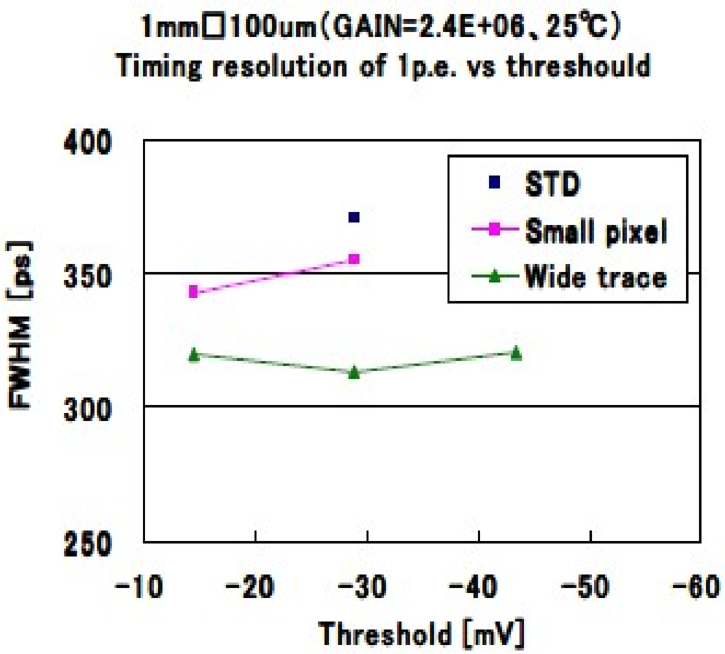

Note:
The steep falling front of the fast peak could be exploited too for optimum timing

$$\sigma_{time}^2 = \frac{\sigma_{amplitude}^2}{N_{samples} \int dt [f'(t)]^2}$$

Signal shape for timing - many photons

Single p.e. signal slow falltime component $\tau_{fall} = R_q\,(C_d+C_d)$

strongly affects multi-photon signal risetime

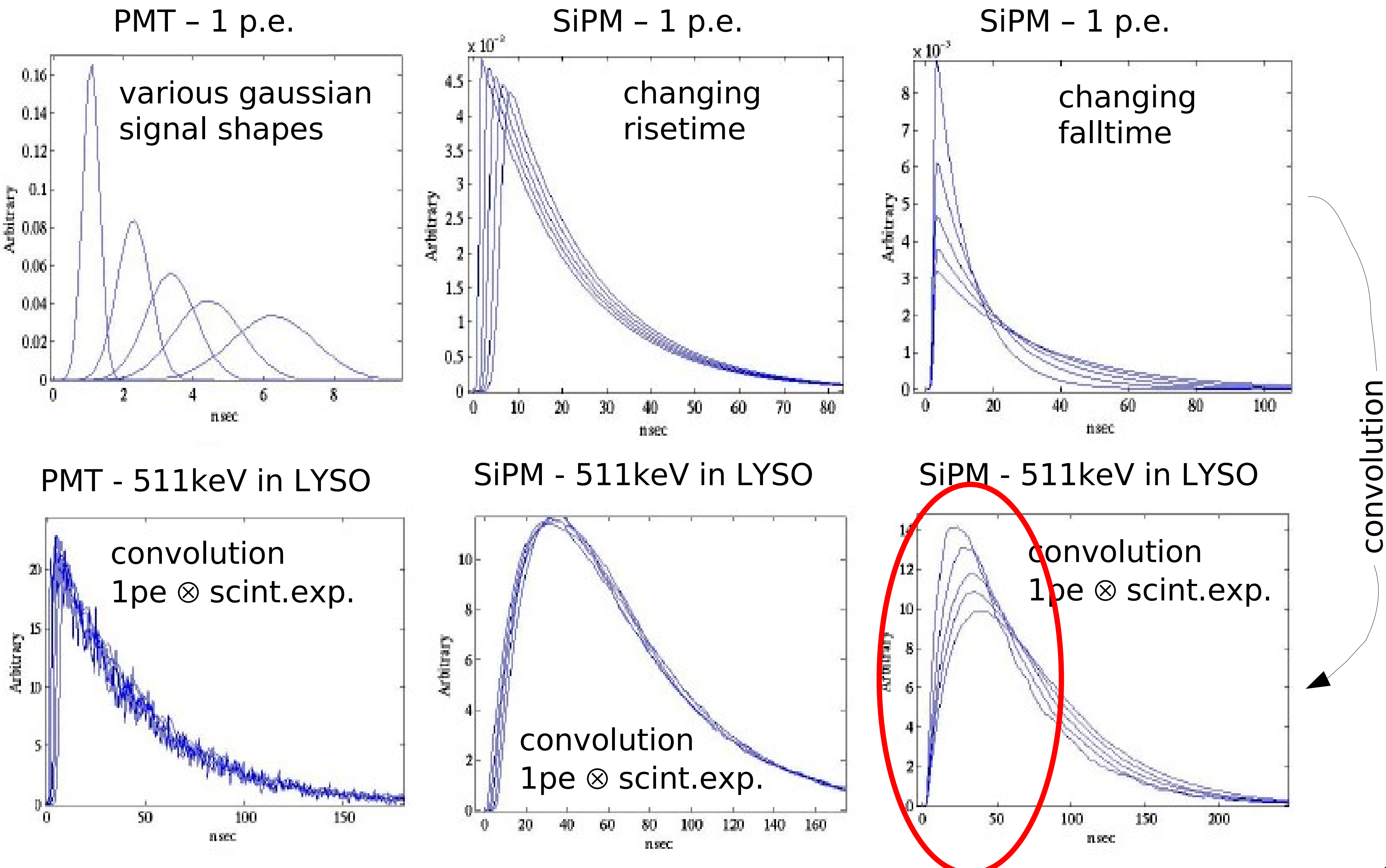

Optimizing shape for timing - many photons

→ peak height ratio $\frac{V^{max}_{fast}}{V^{max}_{slow}} \sim \frac{C_q^2 R_q}{C_d C_{tot} R_{load}}$

Enhancing C_q and R_q does improve timing performances

FBK devices type:

- Active area: 4x4mm^2;
- Cell size: 67x67µm^2;
- Fill factor: 60%;
- C_Q+C_D: about 180fF;
- R_Q: 1.1M;
- Dark noise rate:
  ~100MHz at DV> 4V

C.Piemonte et al IEEE TNS (2011)

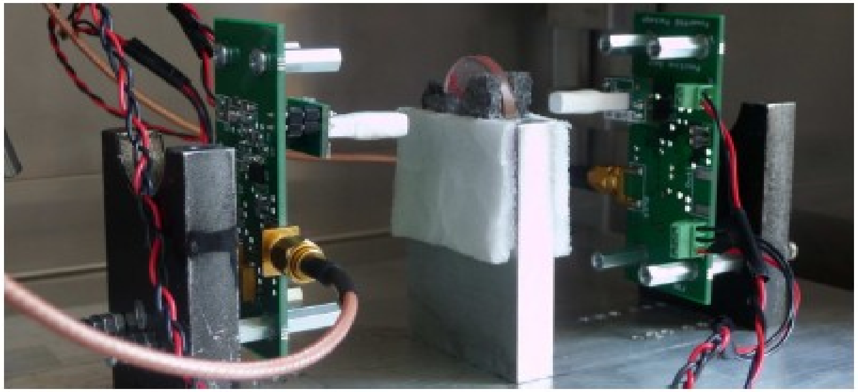

Fig. 2. Test set-up consists of two similar gamma ray detectors (LYSO crystal + SiPM) in coincidence. A [22]Na source (disc in the middle) was used to generate two opposite 511keV photons in coincidence.

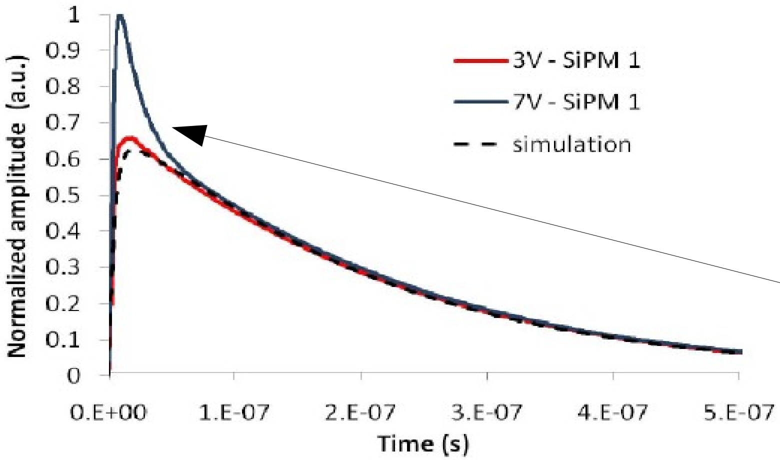

- Signal risetime < 5ns
- CRT ~320ps (*) FWHM triggering at 5% height

Both are much better than for different structures with high C_{tot} and/or lower Cq, Rq (risetime up to several x 10ns, CRT > 400ps)

??? peak shape is not scaling with ΔV
(non linearity in the F.Corsi etal electrical model)
Can be corrected → energy resol. ~11%

(*) ~40% from light propagation in crystals

Conclusions

Properties at low T

- Breakdown V decreases non linearly with T, as expected
  → better stability against T variations than at T room
- Dark rate reduced by several orders of magnitude
  → tunneling mechanism(s) below ~200K
- After-pulsing at % level down to 100K; blow up below 100K
- PDE vs T: modulation up to ±50% wrt T room
  → PDE decr. as T 300K → 250K, incr. as T 250K → 120K, then freeze-out
- PDE vs λ: PDE peaks at lower λ as T decreases
- Cross-talk and Gain (detector capacity) are independent of T (at fixed ΔV)
- Timing resolution improves at low T

SiPMs behave very well at low T, even better than at room T
In the range **100K<T<200K SiPM perform optimally**;
→ excellent alternatives to PMTs in cryogenic applications
(eg LAr, LXe... provided proper changes are made for PDE in XUV...)
→ Optimization for low T (quenching R, ...)

Timing Properties

- Intrinsically ultra-fast devices:
  time to breakdown and jitter < 100ps
- Not negligible non-gaussian tails (ns) for longer wavelengths
- Smaller jitter for blue light than red (depends on the structure)
- Timing improves at low T
- Peculiar pulse shape → device optimization for timing